Brown adipose tissue regulates small artery function through NADPH oxidase 4-derived hydrogen peroxide and redox-sensitive protein kinase G-1α.

Friederich-Persson M, Nguyen Dinh Cat A, Persson P, Montezano AC, Touyz RM.

Institute of Cardiovascular Medicine and Sciences, University of Glasgow, Glasgow, United Kingdom.

Running title: Brown adipose tissue regulates vascular function.

Correspondence:
Rhian M Touyz MBBCh, PhD, FRCP, FRSE.
Institute of Cardiovascular & Medical Sciences
BHF Glasgow Cardiovascular Research Centre
University of Glasgow
126 University Place
Glasgow G12 8TA
Tel: + 44 (0)141 330 7775/7774
Fax: + 44 (0)141 330-3360
Email:Rhian.Touyz@glasgow.ac.uk

Keywords: Vascular function, adipose tissue, contractility

Subject terms: Basic science research, Vascular Biology, Contractile function

TOC category: Basic

TOC subcategory: Vascular Biology

Word count:
Abstract: 249 words
Manuscript: 5 843 words
Number of tables: 1 table
Number of figures: 6 figures, 15 supplemental figures

Abstract

Objective: Biomedical interest in brown adipose tissue (BAT) has increased since the discovery of functionally active BAT in adult humans. While white adipose tissue (WAT) influences vascular function, vascular effects of BAT are elusive. Thus, we investigated the regulatory role and putative vasoprotective effects of BAT, focusing on hydrogen peroxide (H_2O_2), NAPDH-oxidase 4 (Nox4) and redox-sensitive signaling.

Approach/Results: Vascular reactivity was assessed in wild-type (WT) and Nox4-knockout mice ($Nox4^{-/-}$) by wire myography in the absence and presence of perivascular adipose tissue (PVAT) of different phenotypes from various adipose depots: i) mixed WAT/BAT (inguinal adipose tissue (iWAT)), ii) WAT (epididymal visceral fat (EVAT)) and BAT (intrascapular fat). In WT mice, EVAT and PVAT increased EC_{50} to noradrenaline (NA) without affecting maximum contraction. BAT increased EC_{50} and significantly decreased maximum contraction, which were prevented by an H_2O_2 scavenger (PEG-catalase) and a specific PKG-1α inhibitor (DT-3), but not by inhibition of eNOS or guanylate cyclase. BAT induced dimerization of PKG-1α and reduced phosphorylation of myosin light chain phosphatase subunit 1 (MYPT-1) and myosin light chain 20 (MLC-20). BAT from Nox4-knockout mice displayed reduced H_2O_2 levels and no anticontractile effects. PVAT from β3-agonist treated mice displayed browned PVAT and an increased anticontractile effect.

Conclusions: We identify a novel vasoprotective action of BAT through an anticontractile effect that is mechanistically different to WAT. Specifically, BAT, via Nox4-derived H_2O_2, induces PKG-1α activation, resulting in reduced vascular contractility. BAT may constitute an interesting therapeutic target to restore vascular function and prevent vascular complications in cardiovascular diseases.

Abbreviations and Acronyms

5-HT	5-hydroxytryptamine, serotonin
ACh	acetylcholine
BAT	brown adipose tissue
BeAT	beige adipose tissue
BKCa	big conductance calcium sensitive potassium channel
DTT	dithiothreitol
EVAT	epididymal visceral adipose tissue
FBX-10	F-box and leucine-rich repeat protein-10
H_2O_2	hydrogen peroxide
HRP	horse-radish peroxidase
IPO8	importin 8
iWAT	inguinal subcutaneous adipose tissue
K_{Ca}	calcium sensitive potassium channel
KPSS	potassium rich physiological saline solution
L-NAME	NG-nitro-L-arginine methyl ester
MLC	myosin light chain
MYPT1	myosin light chain phosphatase subunit 1
NA	noradrenaline
NADPH	nicotinamide adenine dinucleotide phosphate
Nox	NADPH oxidase
NO	nitric oxide
P2RX5	purinergic Receptor P2X 5
PEG	polyethylene glycated
Phe	phenylephrine
PKG-1	cGMP dependent protein kinase G type-1
PVAT	perivascular adipose tissue
SNP	sodium nitroprusside
SOD	superoxide dismutase
TBX1	T-Box protein 1
Tcf21	transcription factor 21
TEA	tetraethylammonium
TNF-α	tumor necrosis factor-α
TMEM-26	transmembrane protein-26
UBC	ubiquitin C
WAT	white adipose tissue
Zic1	zinc finger of the cerebellum

Introduction

Until recently perivascular adipose tissue (PVAT) was regarded as a structural element responsible for support and mechanical protection of the associated vessel. However, in 1991, Soltis and Cassis demonstrated that PVAT influences vascular function by decreasing contractile responses in rat aorta.[1] PVAT is now widely recognized as a functional regulator of vascular tone through its secretion of relaxing and constricting factors acting on the vasculature. Studies have suggested relaxing factors to be nitric oxide (NO),[2] adiponectin,[2-5] angiotensin 1-7,[6, 7] prostacyclins,[8] hydrogen sulphide (H_2S)[9, 10] and hydrogen peroxide (H_2O_2).[11, 12] These factors are counteracted by contracting factors such as superoxide anion ($O_2^{\cdot-}$),[13] tumor necrosis factor-α (TNF-α) and prostacyclins[14] and the ultimate regulatory effect on vascular tone is reflected by the balance of PVAT-derived vasoconstrictor and vasodilator factors.[15]

The final determinant of vascular contraction is the phosphorylation status of myosin light chain 20 (MLC_{20}), which is regulated by myosin light chain kinase (MLCK) and myosin light chain phosphatase (MLCP). MLCP activity is inhibited by myosin light chain phosphatase regulatory subunit 1 (MYPT1) and MLCK activity is regulated by intracellular calcium (Ca^{2+}) concentration. Counterbalancing vascular contraction is the vasodilatory pathway mediated by cGMP-dependent protein kinase G type 1 (PKG-1).[16] Classically, activation of PKG-1 is mediated via endothelium-dependent increases in cyclic GMP (cGMP), resulting in phosphorylation of big conductance calcium-sensitive potassium channels (BK_{Ca}) and decreased intracellular Ca^{2+}. PKG-1 also phosphorylates RhoA, resulting in reduced Rho kinase (ROCK) activity and consequent reduced phosphorylation of MYPT1. Together, these pathways converge on decreased phosphorylation of MLC_{20} and thereby reduce vascular contraction.[17] Recent studies have also implicated PKG-1 in the anticontractile effects of PVAT.[5, 18]

Adipose tissue comprises two subtypes: white (WAT) and brown (BAT) adipose tissues. WAT is known for its capacity to store lipids and its endocrine role whereas BAT is characterized by energy expenditure in favor of heat generation (non-shivering thermogenesis). Previously thought only to be present in newborns, BAT has recently been identified in adults.[19, 20] In pathologies such as obesity and hypertension, WAT is characterized by low-grade inflammation and is associated with insulin resistance and vascular dysfunction.[21, 22] These changes are also evident in PVAT where the anticontractile effect is lost[23-30] resulting in a pro-contractile phenotype.[23] We previously demonstrated, in experimental models of obesity-related type 2 diabetes, that PVAT-derived factors induce endothelial dysfunction and regulate vascular contractility and remodeling.[31] These processes were associated with increased vascular inflammation and vascular smooth muscle cell proliferation.[32-34]

A major source of both $O_2^{\cdot-}$ and H_2O_2 are the nicotinamide adenine dinucleotide phosphate (NADPH) oxidases (Nox). Seven isoforms with tissue specific expression patterns have been identified and characterized including, Nox1, Nox2, Nox3, Nox4 and Nox5 and the dual oxidases (DUOX) 1 and 2.[35] Nox4 is the predominant isoform expressed in murine and human adipocytes. In adipose tissue however, both Nox2 and Nox4 are expressed at the mRNA level.[36-40] Nox4 produces mainly H_2O_2 whereas the other Nox isoforms produces $O_2^{\cdot-}$. This difference has pathophysiological relevance where H_2O_2-producing Nox4 activity has been shown

to have protective effects on the vasculature whereas $O_2^{\cdot-}$ producing Nox isoforms in many studies are shown to be detrimental.[41, 42] While PVAT of resistance vessels is phenotypically characterized as WAT, the PVAT of the aorta is of a BAT phenotype.[43] Periaortic BAT has anticontractile[1, 26, 44] and anti-inflammatory properties in obesity, and may thus have vasoprotective effects.[43]

In the present study, we examined the role of BAT on vascular function of small resistant arteries and we elucidated some of the underlying molecular mechanisms whereby BAT influences endothelial function and vascular contractility. Our study focuses on small resistance arteries, important in blood pressure regulation and development of hypertension. Arteries were exposed to adipose tissue from different adipose depots epididymal visceral adipose tissue (EVAT), which is phenotypically WAT, inguinal subcutaneous adipose tissue (iWAT) and mesenteric perivascular adipose tissue (PVAT) comprised of both WAT and BAT, and interscapular adipose tissue which is solely BAT.

Materials and methods

Materials and methods are available in the online data supplement.

Results

Phenotyping adipose tissue from different depots.

iWAT, EVAT and mesenteric PVAT are generally characterised as WAT. However, since WAT can convert into a brown-like phenotype, called beige adipose tissue (BeAT), a small amount of BeAT may be present in adipose tissue classically considered as WAT. To confirm the nature of the adipose tissue that we studied, we investigated the adipose phenotype by analyzing mRNA levels of expression of *leptin* and *transcription factor 21 (tcf21)* as markers for WAT, *zinc finger of the cerebellum (Zic1) and purinergic receptor P2X5 (P2RX5)* as specific markers for BAT and *transmembrane protein-26* (*Tmem-26*), *Cd-137*and *T-box protein 1 (Tbx1)* as specific markers for BeAT. *Uncoupling protein-1 (Ucp-1*) and transcription factor *Pat2* are joint markers for both BAT and BeAT. These markers have been previously investigated and evaluated in the phenotyping of adipose tissue.[45, 46]

Interscapular BAT displayed high expression of brown/beige markers UCP-1 and Pat2 as well as the specific markers Zic 1 and P2Rx5 (Supplemental figure I). iWAT expressed brown/beige marker UCP-1 and Pat2 (Supplemental figure I) as well as the specific markers for BeAT TMEM-26, Tbx1 and CD-137 (Supplemental figure II). EVAT displayed only white markers (Supplemental figure III). PVAT displayed expressed WAT specific marker tcf21 as well as BeAT specific marker Tbx-1 and Bat/BeAT marker Pat2 (Supplemental figure II and III). Hence, in our study, we used the paradigm that iWAT and PVAT display a mixed adipose phenotype whereas EVAT is primarily WAT.

BAT exerts an anticontractile effect.

Contractile responses of mouse mesenteric arteries were evaluated using wire myography and showed that the presence of iWAT did not affect vascular contraction in response to increasing doses of noradrenaline (NA) (Figure 1A). The presence of mesenteric PVAT or EVAT increased the sensitivity (EC_{50}) to NA but did not affect maximum contraction to NA (Figure 1B). However, the presence of BAT markedly reduced contraction to NA, phenylephrine (Phe) or serotonine (5-HT), demonstrating a potent anticontractile effect (Figure 1C, Supplemental Figures IV-A and IV-B). The anticontractile effect of BAT was independent of gender and background strain (Supplemental Figures IV-C and IV-D).

H_2O_2 is among the anticontractile factors produced by BAT.

A media transfer approach was used to investigate whether the anticontractile effect of BAT required its immediate localisation to the vessel or if the effect was mediated by a secreted factor. Transfer of media preconditioned with BAT displayed a similar anticontractile effect as BAT directly surrounding the vessel (Figure 1D), indicating the presence of a diffusible factor, secreted by BAT and acting in a paracrine manner. The presence of polyethylene glycated catalase (PEG-catalase), which scavenges H_2O_2, prevented the anticontractile effect of BAT (Figure 2A). Blockade of voltage-gated potassium channels (Kv) by 4-aminopyridine (4-AP) or XE-991, angiotensin 1-7 (Mas) receptors by A779, and production of hydrogen sulphide (H_2S) by β-cyanoalanine did not influence the anticontractile effect of BAT (Supplemental Figure V). Also, endothelial denudation, blockade of production of prostacyclin by indomethacin did not affect the anticontractile effect of BAT (Supplemental figure VI-A and B).

BAT does not influence vascular relaxation.

As demonstrated in supplemental figure VII, endothelium-dependent vascular relaxation in response to acetylcholine (Ach) and endothelium-independent relaxation in response to sodium nitroprusside (SNP) were not affected by BAT.

Nox4 plays a role in BAT-secreted H_2O_2.

As shown in Figure 2, *Nox4* mRNA levels were increased in BAT and iWAT versus iWAT, but not *Nox1* or *Nox2.* Protein expression of Nox4 was increased only in BAT (Supplementary figure VIII-D). Since Nox4 is a constitutively active producer of H_2O_2 we further explored the possibility that Nox4 may be important in vascular tone regulation by BAT-secreted H_2O_2, by studying mice deficient for Nox4 gene ($Nox4^{-/-}$ mice). As shown in Figure 2, H_2O_2 levels in all investigated adipose depots were reduced in $Nox4^{-/-}$ mice (Figure 2B). BAT from $Nox4^{-/-}$ did not exert an anticontractile effect on arteries from wild-type mice (Figure 2C), whilst BAT from wild-type mice exerted an anticontractile effect on arteries from $Nox4^{-/-}$ mice (Figure 2D), demonstrating that the presence of Nox4 in BAT is crucial to induce an anticontractile effect, whereas Nox4 localisation in the vessel does not participate in the anticontractile effect of BAT.

As H_2O_2 may also be sourced from scavenging of $O_2^{\cdot -}$ by superoxide dismutases (SOD) we investigated the expression levels of other Nox enzymes that preferentially produce $O_2^{\cdot -}$ and levels of *Sod* and *catalase* (scavenger of H_2O_2) in BAT. *Nox1* mRNA levels were similar in all adipose depots (Supplementary figure VIII-A) and BAT from mice deleted for Nox1 gene exhibited an anticontractile that was not different from wild-type BAT (Supplemental Figure X). *Nox2* mRNA was lowest in BAT (Supplementary figure VIII-B). *Sod-1* and *Sod-2* mRNA levels were increased in BAT and *catalase* mRNA levels were similar in all depots (Supplemental Figure X). Therefore, although a contribution to total BAT H_2O_2 content from dismutation of $O_2^{\cdot -}$ by *SOD 1-2* cannot be excluded, the $O_2^{\cdot -}$ producing enzymes *Nox1* and *2* do not appear to be major sources of BAT-derived H_2O_2.

BAT influences vascular function through H_2O_2-induced activation of PKG-1.

To investigate molecular mechanisms involved in BAT-induced anticontractility, we focused on cyclic GMP-dependent kinase G (PKG)-1, which is activated by reactive oxygen species (ROS) such as H_2O_2 in vascular smooth muscle cells, and which has been shown to attenuate vasoconstriction and promote vasodilation.[47] The anticontractile effect of BAT was abolished in the presence of a potent and selective inhibitor of PKG-1α (DT-3) (Figure 3A). Similar effects were obtained after selective blockade of BK_{Ca}-channels by iberiotoxin (Figures 3B). The anticontractile effect was also abolished after PKG-inhibitor Rp-8-Br-PET-cGMP and general blockade of Ca^{2+}-sensitive potassium channels by tetraethylammonium (TEA) (Supplementary figure VI – C and D). However, the effect of BAT was similar after blockade of NO synthesis by Nω-Nitro-L-arginine methyl ester hydrochloride (L-NAME) (Figure 3C) or of cGMP production by ODQ (Figure 3D), suggesting that the classical NO-dependent pathway is not involved in mechanisms underlying H_2O_2-induced activation of PKG-1. Previous studies demonstrated that PKG-1 is activated by oxidants, which create a disulphide bond in the enzymatic homodimer.[48] We found that BAT from wild-type mice increased dimerization of PKG-1α but BAT from $Nox4^{-/-}$ mice did not (Figure 4A). Furthermore, dithrioethiol (DTT), a reducing agent, abolished the anticontractile effect of BAT (Supplemental figure XI).
The anticontractile effect of BAT was removed by PEG-catalase and IBTX but not ODQ also with Phe as the contractile agent (Supplementary figure XII). We also investigated the potential role of protein kinase A (PKA) as it may also be activated by oxidants in a similar manner to PKG-1. However, PKA inhibition did not alter the anticontractile effect of BAT (Supplemental Figure XIII).

BAT reduces activation of MYPT1 and MLC-20.

To further confirm the anticontractile effect of BAT, we investigated effects of BAT on the activations of MYPT1 and MLC-20, downstream proteins ultimately responsible for smooth muscle contraction. As shown in Figure 4, incubation of vascular tissue with BAT, resulted in significantly reduced phosphorylation of vascular MYPT1 and MLC_{20} (Figures 4B and 4C).

Differential mechanisms underlie anticontractile effects of WAT and BAT.

We further investigated whether the molecular pathway identified for BAT was also present in mesenteric PVAT. The anticontractile effect of mesenteric PVAT was inhibited by 4-AP but not by PEG-catalase (Supplemental Figure XIV). However, 4-AP did not prevent the anticontractile of BAT (Supplemental figure VI-A), indicating that the anticontractile effects of BAT and mesenteric PVAT are mechanistically different.

Browning of PVAT increases the anticontractile effect through H_2O_2-dependent mechanisms.

To elucidate whether the changing of PVAT phenotype into a BAT/BeAT phenotype affects the anticontractile effect we treated mice with a β_3 agonist, CL-316,243, a well-established method to induce browning in mice.[49] Indeed, β_3-treament increased BAT/BeAT markers in PVAT (Supplementary figure XV) and PVAT from these animals displayed an increased anticontractile effect (Figure 5A). The increased anticontractile effect was reduced but not gone after blockade of H_2O_2 with PEG-catalase and PKG-1α by DT-3 (Figure 5B and C), indicating that the increased anticontractility after browning of resident PVAT is similar in mechanism to that of interscapular BAT.

Discussion

Our study demonstrates that interscapular BAT has anticontractile properties that may be vasoprotective. We elucidated putative novel molecular mechanisms underlying this process and showed that H_2O_2, released from BAT activates vascular PKG-1α through oxidant-induced dimerization. PKG-1α subsequently phosphorylates BK_{Ca} channels and reduces phosphorylation of MYPT1 and MLC-20 with pathways ultimately converging to attenuated vascular contraction. These phenomena are BAT-specific since they did not occur in WAT. Importantly, increased browning of PVAT enhances the anticontractile effect and this increase was shown to be mediated through H_2O_2.and PKG-1α-dependent mechanisms, demonstrating that increasing the amount of resident BAT can affect vascular function on small resistance vessels. Our study concludes that BAT induces a potent anticontractile effect in small resistant arteries through Nox4-dependent mechanism, in particular H_2O_2-induced activation of PKG-1α-dependent signaling.

PVAT of thoracic aorta is primarily a BAT phenotype[43] and has been shown to exert an anticontractile effect, in part through H_2O_2.[1, 26, 44, 50] Gao *et al.* reported that effects of aortic PVAT were prevented by catalase and mimicked by H_2O_2. This study identified two separate pathways of aortic PVAT, an unknown factor inducing endothelium-dependent relaxation and that of H_2O_2 as the endothelium-independent mechanism.[44] It may be suggested that the presence of two mechanisms might reflect the combined effect of both BAT and WAT in aortic PVAT. Mammalian target of rapamycin complex 2 (mToRC2) may be partly responsible for aortic PVAT function. In animals lacking Rapamycin-insensitive companion of mTOR and thus mToRC2, aortic PVAT anticontractility was impaired, possibly mediated through increased levels of inflammatory cytokines TNF-α and interleukin-6.[51] The observed loss of PVAT function was still evident in denuded arteries, supporting an

endothelial-independent mechanism for aortic brown PVAT which is in accordance with the present study where endothelial denudation did not eliminate the anticontractile effect of BAT.

The central player in our described mechanism, H_2O_2, has been the focus of intense research and its role in the vasculature has been extensively reviewed.[52, 53] In the vasculature, H_2O_2 has been suggested to have both detrimental[54] and protective effects[41]. These conflicting results may be due to differences in sub-cellular localization of H_2O_2 and other ROS and may relate in part to different cell types preferentially producing H_2O_2.[55, 56] In the present study, H_2O_2 mediates a protective role, activating PKG-1α, ultimately resulting in reduced vascular contraction. H_2O_2 can originate from the dismutation of $O_2^{\cdot-}$ by SOD but also from a dedicated H_2O_2-producer: Nox4. Due to its vascular localization,[57] constitutively active function and production of H_2O_2, Nox4 is generally regarded as a vaso-protective Nox. Indeed, it is highly expressed in BAT and pivotal to the anticontractile effect we observed, as BAT from Nox4$^{-/-}$ mice failed to exhibit a vascular effect. However, BAT from wild-type mice mediated an anticontractile effect on vessels from Nox4$^{-/-}$ mice, suggesting that the perivascular production of H_2O_2 is critical for the anticontractile effect of BAT, rather than H_2O_2 produced locally in smooth muscle cells in the vascular media. - Also, the need for a threshold level of H_2O_2 is evident as the H_2O_2 levels were reduced but not abolished in adipose tissue from Nox4$^{-/-}$ mice despite the anticontractile effect being abrogated. Importantly, we have previously shown that Nox4 is expressed in human adipocytes.[58]

In the present study, vessels devoid of PVAT from Nox4$^{-/-}$ mice displayed increased contraction and BAT from these mice lacked an anticontractile effect. However, Nox4$^{-/-}$ mice display similar blood pressure as wildtype mice under basal conditions and after angiotensin II infusion[41] and basal blood pressure is reduced only after endothelial overexpression of Nox4.[59] Taken together, this suggests that Nox4 may not be a critical regulator of of blood pressure under basal conditions but may be important for blood pressure regulation in conditions were it is increased.

Whether BAT-derived H_2O_2 mediates an anticontractile effect or is determined by downstream signalling through PKG-1α remains unclear. Importantly, H_2O_2 is known to activate PKG-1α by oxidizing cysteine residues, creating a disulphide bond between the PKG-1α homodimers. Subsequently, there is a conformational change that exposes the phosphorylation site and downstream signalling occurs. Eaton *et al.* demonstrated that mice that do not activate PKG-1α in this manner, become hypertensive under normal conditions,[48] demonstrating the importance of the H_2O_2-PKG-1α signalling axis in regulating normal blood pressure. In our study, BAT induced dimerization of PKG-1α but when dimerization was prevented by DTT the anticontractile effect was abolished. Interestingly, blockade of H_2O_2 to PKG-1α signalling by DTT revealed a pro-contractile effect of BAT, suggesting that when the beneficial part of H_2O_2-dependent signalling is removed, remaining signalling or other pro-contractile factors such as $O_2^{\cdot-}$ can exert a vascular contractile action.

In our study, blockade of PKG-1α itself or its downstream target, BK_{Ca} channels, attenuated the anticontractile effect of BAT. This is in accordance with previous studies implicating the BK_{Ca} channels as mediators of the anticontractile effect of adipose tissue.[5] Importantly, Withers *et al.* found the anticontractile effect of PVAT to be absent in mice lacking PKG-1.[18]

Our study highlights the fact that various adipose depots have anticontractile properties but that underlying molecular mechanisms may differ. Previous studies of mesenteric PVAT reported the involvement of voltage-gated K-channels (Kv),[60, 61] in some cases further specifying it to KCNQ (Kv-7)-channels.[9] In the present study, the effect of mesenteric PVAT was inhibited by a Kv channel blocker but the anticontractile effect of BAT was not affected. Similarly, scavenging of H_2O_2 removed the anticontractile effect of BAT but had no effect on mesenteric PVAT. Additionally, inhibition of mechanisms previously shown to be involved in vasoprotective effects of PVAT such as H_2S, NO, prostacyclins and angiotensin 1-7 had no effect on the anticontractile effect of BAT. Taken together, these findings suggest that the anticontractile processes of mesenteric PVAT and BAT involve distinct signaling pathways. However, it should also be highlighted that mesenteric PVAT could be mediated by the small degree of BAT or BeAT within the depots commonly characterized as white.[62] Originating from white adipocytes[63] inactive beige adipocytes localized within WAT can be mobilised into BeAT by exposure to cold or stimulation of β_3-receptors, resulting in a process called browning. Importantly, BeAT is morphologically and functionally similar to classical brown adipocytes.[64]

Our phenotyping revealed that while EVAT was characterized as WAT, both PVAT and iWAT displayed BeAT markers and were thus characterized as a mix of WAT and BeAT. Interestingly, iWAT did not display an anticontractile effect and the anticontractile effect of PVAT was not affected by PEG-catalase. Either BeAT does not behave in a similar manner to BAT in terms of vascular effect, or a critical level of BAT or BeAT needs to be present before the anticontractile effect is functional. To investigate if an increased amount of BeAT may also exert an anticontractile effect we induced browning through a β3-agonist. In these mice, PVAT displayed an increased anticontractile effect compared to PVAT from controls, an effect that was sensitive to both scavenging of H_2O_2 and blockade of PKG-1α, suggesting that the mechanisms of BAT and BeAT may indeed be similar if a critical threshold of BeAT is reached. BAT did not affect vascular relaxation and may relate to the fact that the NOS-NO pathway was not influenced by BAT.

From a pathophysiological viewpoint, our findings may be important since several clinical and experimental studies have reported the loss of the PVAT anticontractile effect in obesity, type 2 diabetes[27-29] and hypertension.[23-26] Patients after bariatric surgery displayed improved insulin sensitivity, reduced blood pressure and a restored anticontractile effect of PVAT.[2] Interestingly, BAT surrounding the aorta has been reported to be resistant to obesity-induced inflammation, suggesting that BAT may help to protect the vasculature during pathological conditions. Furthermore, transplantation of BAT into the visceral cavity corrects the metabolic phenotype of rodents with diabetes and metabolic syndrome and transplantation of BAT has been suggested to be of future importance in metabolic diseases.[65-67] Based on the novel results of our study, BAT clearly demonstrates a redox-sensitive vasoprotective effect and as such exposing small arteries to BAT, or increased browning of PVAT, may be an interesting strategy to improve vascular function in pathological conditions.

In conclusion, Nox4 in BAT produces H_2O_2, leading to oxidant-induced activation of PKG-1α and its downstream pathway. This pathway ultimately converges to influence signaling that decreases phosphorylation of MYPT1 and MLC-20, with consequent reduced vascular contraction. Further, we show that browning of PVAT

is feasible, and identify an anticontractile effect through BAT-mediated processes. Our study provides new insights into mechanisms whereby BAT may exert vasoprotective effects as summarized in Figure 6. These findings have clinical significance as a novel therapeutic target, because PVAT-enriched with BAT may preserve vascular function and prevent vascular complications in pathologies such as hypertension, obesity and metabolic syndrome.

Acknowledgements

A) **Acknowledgements:** Craig Daly and Laura McPherson (University of Glasgow) are thanked for technical assistance. Katrin Schroder and Ralf Brandes (Goethe-Universitat, Frankfurt) are thanked for supplying the Nox4$^{-/-}$ mice.
B) **Sources of funding**: This work was supported by grants from the British Heart Foundation (BHF) (RG/13/7/30099; RE/13/5/30177). RMT was supported through a BHF Chair (CH/12/429762). MFP was supported through a postdoctoral fellowship from the Wenner-Gren Foundations, Stockholm, Sweden. PP was supported by the Swedish Heart and Lung Foundation and the Swedish Society for Medical Research.
C) **Disclosures:** The authors have nothing to disclose.

References

1. Soltis EE, Cassis LA. Influence of perivascular adipose tissue on rat aortic smooth muscle responsiveness. *Clinical and experimental hypertension. Part A, Theory and practice*. 1991;13:277-296
2. Aghamohammadzadeh R, Greenstein AS, Yadav R, Jeziorska M, Hama S, Soltani F, Pemberton PW, Ammori B, Malik RA, Soran H, Heagerty AM. Effects of bariatric surgery on human small artery function: Evidence for reduction in perivascular adipocyte inflammation, and the restoration of normal anticontractile activity despite persistent obesity. *Journal of the American College of Cardiology*. 2013;62:128-135
3. Weston AH, Egner I, Dong Y, Porter EL, Heagerty AM, Edwards G. Stimulated release of a hyperpolarizing factor (adhf) from mesenteric artery perivascular adipose tissue: Involvement of myocyte bkca channels and adiponectin. *British journal of pharmacology*. 2013;169:1500-1509
4. Fesus G, Dubrovska G, Gorzelniak K, Kluge R, Huang Y, Luft FC, Gollasch M. Adiponectin is a novel humoral vasodilator. *Cardiovascular research*. 2007;75:719-727
5. Lynch FM, Withers SB, Yao Z, Werner ME, Edwards G, Weston AH, Heagerty AM. Perivascular adipose tissue-derived adiponectin activates bk(ca) channels to induce anticontractile responses. *Am J Physiol Heart Circ Physiol*. 2013;304:H786-795
6. Lee RM, Bader M, Alenina N, Santos RA, Gao YJ, Lu C. Mas receptors in modulating relaxation induced by perivascular adipose tissue. *Life sciences*. 2011;89:467-472
7. Lee RM, Lu C, Su LY, Gao YJ. Endothelium-dependent relaxation factor released by perivascular adipose tissue. *Journal of hypertension*. 2009;27:782-790
8. Chang L, Villacorta L, Li R, Hamblin M, Xu W, Dou C, Zhang J, Wu J, Zeng R, Chen YE. Loss of perivascular adipose tissue on peroxisome proliferator-activated receptor-gamma deletion in smooth muscle cells impairs intravascular thermoregulation and enhances atherosclerosis. *Circulation*. 2012;126:1067-1078
9. Schleifenbaum J, Kohn C, Voblova N, Dubrovska G, Zavarirskaya O, Gloe T, Crean CS, Luft FC, Huang Y, Schubert R, Gollasch M. Systemic peripheral artery relaxation by kcnq channel openers and hydrogen sulfide. *Journal of hypertension*. 2010;28:1875-1882

10. Fang L, Zhao J, Chen Y, Ma T, Xu G, Tang C, Liu X, Geng B. Hydrogen sulfide derived from periadventitial adipose tissue is a vasodilator. *Journal of hypertension*. 2009;27:2174-2185
11. Miura H, Bosnjak JJ, Ning G, Saito T, Miura M, Gutterman DD. Role for hydrogen peroxide in flow-induced dilation of human coronary arterioles. *Circ Res*. 2003;92:e31-40
12. Thengchaisri N, Kuo L. Hydrogen peroxide induces endothelium-dependent and -independent coronary arteriolar dilation: Role of cyclooxygenase and potassium channels. *Am J Physiol Heart Circ Physiol*. 2003;285:H2255-2263
13. Gao YJ, Takemori K, Su LY, An WS, Lu C, Sharma AM, Lee RM. Perivascular adipose tissue promotes vasoconstriction: The role of superoxide anion. *Cardiovascular research*. 2006;71:363-373
14. Meyer MR, Fredette NC, Barton M, Prossnitz ER. Regulation of vascular smooth muscle tone by adipose-derived contracting factor. *PLoS One*. 2013;8:e79245
15. Brown NK, Zhou Z, Zhang J, Zeng R, Wu J, Eitzman DT, Chen YE, Chang L. Perivascular adipose tissue in vascular function and disease: A review of current research and animal models. *Arterioscler Thromb Vasc Biol*. 2014;34:1621-1630
16. Kimura K, Ito M, Amano M, Chihara K, Fukata Y, Nakafuku M, Yamamori B, Feng J, Nakano T, Okawa K, Iwamatsu A, Kaibuchi K. Regulation of myosin phosphatase by rho and rho-associated kinase (rho-kinase). *Science*. 1996;273:245-248
17. Mahavadi S, Nalli A, Al-Shboul O, Murthy KS. Inhibition of mlc20 phosphorylation downstream of ca2+ and rhoa: A novel mechanism involving phosphorylation of myosin phosphatase interacting protein (m-rip) by pkg and stimulation of mlc phosphatase activity. *Cell biochemistry and biophysics*. 2014;68:1-8
18. Withers SB, Simpson L, Fattah S, Werner ME, Heagerty AM. Cgmp-dependent protein kinase (pkg) mediates the anticontractile capacity of perivascular adipose tissue. *Cardiovascular research*. 2014;101:130-137
19. Cypess AM, Lehman S, Williams G, Tal I, Rodman D, Goldfine AB, Kuo FC, Palmer EL, Tseng YH, Doria A, Kolodny GM, Kahn CR. Identification and importance of brown adipose tissue in adult humans. *N Engl J Med*. 2009;360:1509-1517
20. Virtanen KA, Lidell ME, Orava J, Heglind M, Westergren R, Niemi T, Taittonen M, Laine J, Savisto NJ, Enerback S, Nuutila P. Functional brown adipose tissue in healthy adults. *N Engl J Med*. 2009;360:1518-1525
21. Nishimura S, Manabe I, Nagai R. Adipose tissue inflammation in obesity and metabolic syndrome. *Discovery medicine*. 2009;8:55-60
22. Berg AH, Scherer PE. Adipose tissue, inflammation, and cardiovascular disease. *Circ Res*. 2005;96:939-949
23. Gao YJ. Dual modulation of vascular function by perivascular adipose tissue and its potential correlation with adiposity/lipoatrophy-related vascular dysfunction. *Current pharmaceutical design*. 2007;13:2185-2192
24. Galvez-Prieto B, Dubrovska G, Cano MV, Delgado M, Aranguez I, Gonzalez MC, Ruiz-Gayo M, Gollasch M, Fernandez-Alfonso MS. A reduction in the amount and anti-contractile effect of periadventitial mesenteric adipose tissue precedes hypertension development in spontaneously hypertensive rats. *Hypertension research : official journal of the Japanese Society of Hypertension*. 2008;31:1415-1423
25. Galvez-Prieto B, Somoza B, Gil-Ortega M, Garcia-Prieto CF, de Las Heras AI, Gonzalez MC, Arribas S, Aranguez I, Bolbrinker J, Kreutz R, Ruiz-Gayo M, Fernandez-Alfonso MS. Anticontractile effect of perivascular adipose tissue and leptin are reduced in hypertension. *Frontiers in pharmacology*. 2012;3:103
26. Ma L, Ma S, He H, Yang D, Chen X, Luo Z, Liu D, Zhu Z. Perivascular fat-mediated vascular dysfunction and remodeling through the ampk/mtor pathway in high-fat diet-induced obese rats. *Hypertension research : official journal of the Japanese Society of Hypertension*. 2010;33:446-453

27. Greenstein AS, Khavandi K, Withers SB, Sonoyama K, Clancy O, Jeziorska M, Laing I, Yates AP, Pemberton PW, Malik RA, Heagerty AM. Local inflammation and hypoxia abolish the protective anticontractile properties of perivascular fat in obese patients. *Circulation*. 2009;119:1661-1670
28. Gil-Ortega M, Condezo-Hoyos L, Garcia-Prieto CF, Arribas SM, Gonzalez MC, Aranguez I, Ruiz-Gayo M, Somoza B, Fernandez-Alfonso MS. Imbalance between pro and anti-oxidant mechanisms in perivascular adipose tissue aggravates long-term high-fat diet-derived endothelial dysfunction. *PLoS One*. 2014;9:e95312
29. Marchesi C, Ebrahimian T, Angulo O, Paradis P, Schiffrin EL. Endothelial nitric oxide synthase uncoupling and perivascular adipose oxidative stress and inflammation contribute to vascular dysfunction in a rodent model of metabolic syndrome. *Hypertension*. 2009;54:1384-1392
30. Virdis A, Duranti E, Rossi C, Dell'Agnello U, Santini E, Anselmino M, Chiarugi M, Taddei S, Solini A. Tumour necrosis factor-alpha participates on the endothelin-1/nitric oxide imbalance in small arteries from obese patients: Role of perivascular adipose tissue. *European heart journal*. 2015;36:784-794
31. Briones AM, Nguyen Dinh Cat A, Callera GE, Yogi A, Burger D, He Y, Correa JW, Gagnon AM, Gomez-Sanchez CE, Gomez-Sanchez EP, Sorisky A, Ooi TC, Ruzicka M, Burns KD, Touyz RM. Adipocytes produce aldosterone through calcineurin-dependent signaling pathways: Implications in diabetes mellitus-associated obesity and vascular dysfunction. *Hypertension*. 2012;59:1069-1078
32. Chatterjee TK, Stoll LL, Denning GM, Harrelson A, Blomkalns AL, Idelman G, Rothenberg FG, Neltner B, Romig-Martin SA, Dickson EW, Rudich S, Weintraub NL. Proinflammatory phenotype of perivascular adipocytes: Influence of high-fat feeding. *Circ Res*. 2009;104:541-549
33. Chatterjee TK, Aronow BJ, Tong WS, Manka D, Tang Y, Bogdanov VY, Unruh D, Blomkalns AL, Piegore MG, Jr., Weintraub DS, Rudich SM, Kuhel DG, Hui DY, Weintraub NL. Human coronary artery perivascular adipocytes overexpress genes responsible for regulating vascular morphology, inflammation, and hemostasis. *Physiological genomics*. 2013;45:697-709
34. Rajsheker S, Manka D, Blomkalns AL, Chatterjee TK, Stoll LL, Weintraub NL. Crosstalk between perivascular adipose tissue and blood vessels. *Curr Opin Pharmacol*. 2010;10:191-196
35. Drummond GR, Selemidis S, Griendling KK, Sobey CG. Combating oxidative stress in vascular disease: Nadph oxidases as therapeutic targets. *Nature reviews. Drug discovery*. 2011;10:453-471
36. Han CY, Umemoto T, Omer M, Den Hartigh LJ, Chiba T, LeBoeuf R, Buller CL, Sweet IR, Pennathur S, Abel ED, Chait A. Nadph oxidase-derived reactive oxygen species increases expression of monocyte chemotactic factor genes in cultured adipocytes. *The Journal of biological chemistry*. 2012;287:10379-10393
37. Nishimura S, Manabe I, Nagasaki M, Eto K, Yamashita H, Ohsugi M, Otsu M, Hara K, Ueki K, Sugiura S, Yoshimura K, Kadowaki T, Nagai R. Cd8+ effector t cells contribute to macrophage recruitment and adipose tissue inflammation in obesity. *Nature medicine*. 2009;15:914-920
38. Mouche S, Mkaddem SB, Wang W, Katic M, Tseng YH, Carnesecchi S, Steger K, Foti M, Meier CA, Muzzin P, Kahn CR, Ogier-Denis E, Szanto I. Reduced expression of the nadph oxidase nox4 is a hallmark of adipocyte differentiation. *Biochimica et biophysica acta*. 2007;1773:1015-1027
39. Mahadev K, Motoshima H, Wu X, Ruddy JM, Arnold RS, Cheng G, Lambeth JD, Goldstein BJ. The nad(p)h oxidase homolog nox4 modulates insulin-stimulated generation of h2o2 and plays an integral role in insulin signal transduction. *Molecular and cellular biology*. 2004;24:1844-1854

40. Ronn T, Volkov P, Gillberg L, Kokosar M et al. Impact of age, bmi and hba1c levels on the genome-wide DNA methylation and mrna expression patterns in human adipose tissue and identification of epigenetic biomarkers in blood. *Human molecular genetics*. 2015;24:3792-3813
41. Schroder K, Zhang M, Benkhoff S, Mieth A, Pliquett R, Kosowski J, Kruse C, Luedike P, Michaelis UR, Weissmann N, Dimmeler S, Shah AM, Brandes RP. Nox4 is a protective reactive oxygen species generating vascular nadph oxidase. *Circ Res*. 2012;110:1217-1225
42. Cave AC, Brewer AC, Narayanapanicker A, Ray R, Grieve DJ, Walker S, Shah AM. Nadph oxidases in cardiovascular health and disease. *Antioxidants & redox signaling*. 2006;8:691-728
43. Fitzgibbons TP, Kogan S, Aouadi M, Hendricks GM, Straubhaar J, Czech MP. Similarity of mouse perivascular and brown adipose tissues and their resistance to diet-induced inflammation. *Am J Physiol Heart Circ Physiol*. 2011;301:H1425-1437
44. Gao YJ, Lu C, Su LY, Sharma AM, Lee RM. Modulation of vascular function by perivascular adipose tissue: The role of endothelium and hydrogen peroxide. *British journal of pharmacology*. 2007;151:323-331
45. Garcia RA, Roemmich JN, Claycombe KJ. Evaluation of markers of beige adipocytes in white adipose tissue of the mouse. *Nutrition & metabolism*. 2016;13:24
46. de Jong JM, Larsson O, Cannon B, Nedergaard J. A stringent validation of mouse adipose tissue identity markers. *American journal of physiology. Endocrinology and metabolism*. 2015;308:E1085-1105
47. Burgoyne JR, Madhani M, Cuello F, Charles RL, Brennan JP, Schroder E, Browning DD, Eaton P. Cysteine redox sensor in pkgia enables oxidant-induced activation. *Science*. 2007;317:1393-1397
48. Prysyazhna O, Rudyk O, Eaton P. et al. Effect of cl-316,243, a thermogenic beta 3-agonist, on energy balance and brown and white adipose tissues in rats. *Am J Physiol*. 1994;266:R1371-1382
50. Spradley FT, Ho DH, Pollock JS. Dahl ss rats demonstrate enhanced aortic perivascular adipose tissue-mediated buffering of vasoconstriction through activation of nos in the endothelium. *American journal of physiology. Regulatory, integrative and comparative physiology*. 2016;310:R286-296
51. Bhattacharya I, Gotfried MH, Ji AJ, Saunders JP, Gourley I, Diehl A, Korth-Bradley JM. Reassessment of tigecycline bone concentrations in volunteers undergoing elective orthopedic procedures. *Journal of clinical pharmacology*. 2014;54:70-74
52. Konior A, Schramm A, Czesnikiewicz-Guzik M, Guzik TJ. Nadph oxidases in vascular pathology. *Antioxidants & redox signaling*. 2014;20:2794-2814
53. Takac I, Schroder K, Brandes RP. The nox family of nadph oxidases: Friend or foe of the vascular system? *Current hypertension reports*. 2012;14:70-78
54. Kleinschnitz C, Grund H, Wingler K et al. Post-stroke inhibition of induced nadph oxidase type 4 prevents oxidative stress and neurodegeneration. *PLoS biology*. 2010;8
55. Touyz RM, Montezano AC. Vascular nox4: A multifarious nadph oxidase. *Circ Res*. 2012;110:1159-1161
56. Schmidt HH, Wingler K, Kleinschnitz C, Dusting G. Nox4 is a janus-faced reactive oxygen species generating nadph oxidase. *Circ Res*. 2012;111:e15-16; author reply e17-18
57. Sorescu D, Weiss D, Lassegue B, Clempus RE, Szocs K, Sorescu GP, Valppu L, Quinn MT, Lambeth JD, Vega JD, Taylor WR, Griendling KK. Superoxide production and expression of nox family proteins in human atherosclerosis. *Circulation*. 2002;105:1429-1435
58. Rios FJ, Neves KB, Nguyen Dinh Cat A, Even S, Palacios R, Montezano AC, Touyz RM. Cholesteryl ester-transfer protein inhibitors stimulate aldosterone biosynthesis in adipocytes through nox-dependent processes. *J Pharmacol Exp Ther*. 2015;353:27-34

59. Ray R, Murdoch CE, Wang M et al. Endothelial nox4 nadph oxidase enhances vasodilatation and reduces blood pressure in vivo. *Arteriosclerosis, thrombosis, and vascular biology*. 2011;31:1368-1376
60. Galvez B, de Castro J, Herold D, Dubrovska G, Arribas S, Gonzalez MC, Aranguez I, Luft FC, Ramos MP, Gollasch M, Fernandez Alfonso MS. Perivascular adipose tissue and mesenteric vascular function in spontaneously hypertensive rats. *Arterioscler Thromb Vasc Biol*. 2006;26:1297-1302
61. Verlohren S, Dubrovska G, Tsang SY, Essin K, Luft FC, Huang Y, Gollasch M. Visceral periadventitial adipose tissue regulates arterial tone of mesenteric arteries. *Hypertension*. 2004;44:271-276
62. Wu J, Bostrom P, Sparks LM et al. Beige adipocytes are a distinct type of thermogenic fat cell in mouse and human. *Cell*. 2012;150:366-376
63. Hummelsheim H, Wiesendanger M. Is the hindlimb representation of the rat's cortex a 'sensorimotor amalgam'? *Brain research*. 1985;346:75-81
64. Lee P, Werner CD, Kebebew E, Celi FS. Functional thermogenic beige adipogenesis is inducible in human neck fat. *International journal of obesity*. 2014;38:170-176
65. Stanford KI, Middelbeek RJ, Townsend KL, An D, Nygaard EB, Hitchcox KM, Markan KR, Nakano K, Hirshman MF, Tseng YH, Goodyear LJ. Brown adipose tissue regulates glucose homeostasis and insulin sensitivity. *J Clin Invest*. 2013;123:215-223
66. Liu X, Wang S, You Y et al. Brown adipose tissue transplantation reverses obesity in ob/ob mice. *Endocrinology*. 2015;156:2461-2469
67. Gunawardana SC, Piston DW. Insulin-independent reversal of type 1 diabetes in nonobese diabetic mice with brown adipose tissue transplant. *Am J Physiol Endocrinol Metab*. 2015;308:E1043-1055

Highlights

- Vascular dysfunction is common feature in hypertension, diabetes and obesity and PVAT has emerged as an important regulator of vascular function.
- The present study demonstrates that BAT can modulate the function of small resistance vessels. This anticontractile effect is higher than the one induced by PVAT in physiological conditions.
- The mechanisms identified include Nox4-derived H_2O_2 from BAT which activates PKG-1α and its downstream pathways, resulting in reduced vascular contraction.
- By clearly elucidating the mechanisms of how BAT influences vascular tone, our findings provide a rationale to target BAT for new therapeutic strategies aiming to preserve vascular function and to prevent vascular complications in cardiovascular diseases such as diabetes, obesity and hypertension.

Figure legends

Figure 1. A) iWAT does not affect vascular contraction in response to NA. B) EVAT and mesenteric PVAT increase EC_{50} in response to NA. C) BAT increases EC_{50} and reduces MC in response to NA, demonstrating a potent anticontractile effect. D) The anticontractile effect of BAT is mediated by a transferrable factor. Values are

expressed as means±SD. In brackets are indicated the number of animals per group. Repeated measured one-way ANOVA followed by Bonferroni multiple comparison test, or Student's t-test were appropriate. * denotes P<0.05. BAT: brown adipose tissue; EC: effective concentration; EVAT: epididymal visceral adipose tissue; iWAT: inguinal subcutaneous white adipose tissue; KPSS: potassium-rich physiological saline solution; MC: maximal contraction; NA: noradrenaline; PVAT: mesenteric perivascular adipose tissue.

Figure 2. A) Presence of PEG-catalase prevents the anticontractile effect of BAT. 2by2 interaction: p<0.05. B) H_2O_2 levels are decreased in all adipose depots from NOX4$^{-/-}$ mice. C) BAT from Nox4$^{-/-}$ mice does not exert an anticontractile effect. 2by2 interaction: ns. D) BAT from wild-type exerts an anticontractile effect regardless if the vessel is from wild-type or Nox4$^{-/-}$ animals. 2by2 interaction: ns.
Values are expressed as means±SD. In brackets are indicated the number of animals per group. Repeated measured two-way ANOVA, followed by Bonferroni multiple comparison test * denotes P<0.05 vs. clean vessels. In B - n=6 animals per group. One-way ANOVA, followed by Bonferroni multiple comparison test, * P<0.05 vs. wildtype within the tissue, # denotes P<0.05 vs. EVAT. BAT: brown adipose tissue; EVAT: epididymal visceral adipose tissue; iWAT: inguinal white adipose tissue; H_2O_2: hydrogen peroxide, KPSS: potassium-rich physiological saline solution, NA: noradrenaline; Nox4: NADPH oxidase 4; PVAT: perivascular adipose tissue.

Figure 3. A) The anticontractile effect of BAT is blocked by PKG-1α selective inhibitor DT-3 (2by2 interaction: p<0.05) and B) the selective BK_{Ca} channel blocker IBTX (2by2 interaction: p<0.05). C) The anticontractile effect is not affected NOS-inhibitor L-NAME (2by2 interaction: ns) or by soluble guanylate cyclase inhibitor ODQ (D, 2by2 interaction: p<0.05). Values are expressed as means±SD. In brackets are indicated the number of animals per group. Repeated measured two-way ANOVA, followed by Bonferroni multiple comparison test, * denotes P<0.05 vs. clean vessels. BAT: brown adipose tissue; BK_{Ca}: big conductance calcium-sensitive potassium channel; IBTX: iberiotoxin; K_{Ca}: calcium-sensitive potassium channel; KPSS: potassium-rich physiological saline solution; L-NAME: Nω-Nitro-L-arginine methyl ester hydrochloride; NA: noradrenaline.

Figure 4. A) Dimerization of PKG-1α is induced by BAT from wild-type mice but not by BAT from Nox4$^{-/-}$ mice. (B) Phosphorylation of MYPT1 and MLC_{20} (C) is decreased by BAT from wild-type mice WT but not with BAT from Nox4$^{-/-}$ mice. Values are expressed as means±SD. n=4-6 animals per group. One-way ANOVA, followed by Bonferroni multiple comparison test, * denotes P<0.05 vs. clean. BAT: brown adipose tissue; DTT: dithioethriethol; H_2O_2: hydrogen peroxide; MLC_{20}: myosin light chain 20; MYPT1: myosin light chain phosphatase regulatory subunit 1; Nox4: NADPH oxidase 4.

Figure 5. A) Browning of PVAT increases the anticontractile effect (2by2 interaction: p<0.05 B). The anticontractile effect in the β3-agonist treated mice is diminished by PEG-catalase (2by2 interaction: p<0.05) and by C) PKG-Iα inhibitor DT-3 (2by2 interaction: p<0.05). Values are expressed as means±SD. In brackets are indicated the number of animals per group. Repeated measured two-way ANOVA, followed by Bonferroni multiple comparison test, * denotes P<0.05 vs. clean vessels. KPSS:

potassium-rich physiological saline solution; NA: noradrenaline; PEG: polyethyleneglykol; PVAT: perivascular adipose tissue.

Figure 6. Summarized scheme of proposed mechanisms whereby BAT may induce vasoprotective effects. BK_{Ca}: big conductance calcium-sensitive potassium channel; cGMP: cyclic GMP; DTT: dithioethrethiol; eNOS: endothelial nitric oxide synthase; H_2O_2: hydrogen peroxide; MLC: myosin light chain; MLCK: myosin light chain kinase; MLCP: myosin light chain phosphatase; MYPT1: myosin light chain phosphatase regulatory subunit 1; NO: nitric oxide; Nox4: NADPHoxidase 4; ROCK: Rho kinase; sGC: soluble guanylate cyclase; TEA: tetraethylammonium; VDCC: voltage dependent calcium channel.

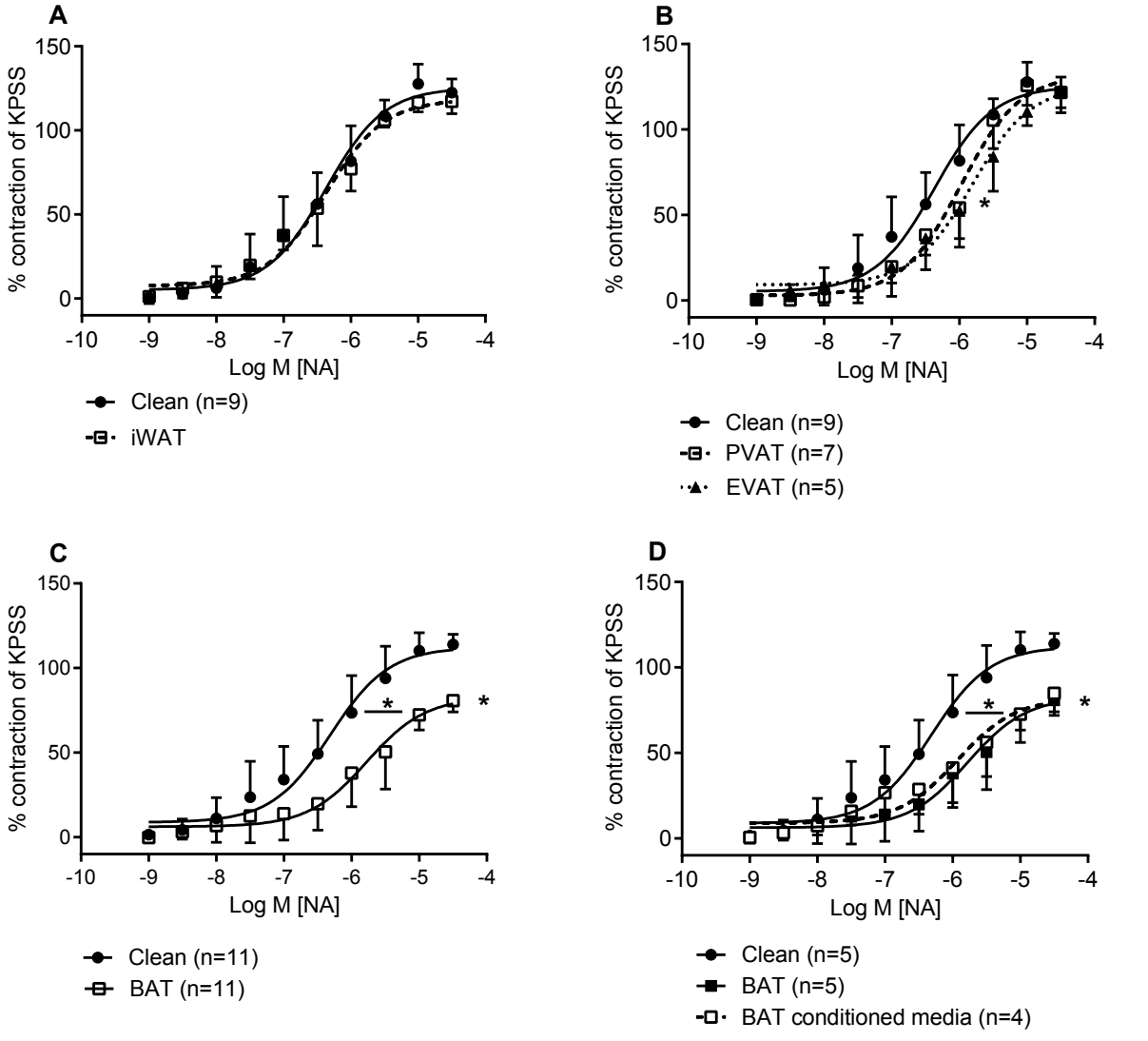
A
% contraction of KPSS
150
100
50
0
-10
-9
-8
-7
-6
-5
-4
Log M [NA]
Clean (n=9)
iWAT
B
% contraction of KPSS
Log M [NA]
*
Clean (n=9)
PVAT (n=7)
EVAT (n=5)
C
% contraction of KPSS
Log M [NA]
*
*
Clean (n=11)
BAT (n=11)
D
% contraction of KPSS
Log M [NA]
*
*
Clean (n=5)
BAT (n=5)
BAT conditioned media (n=4)

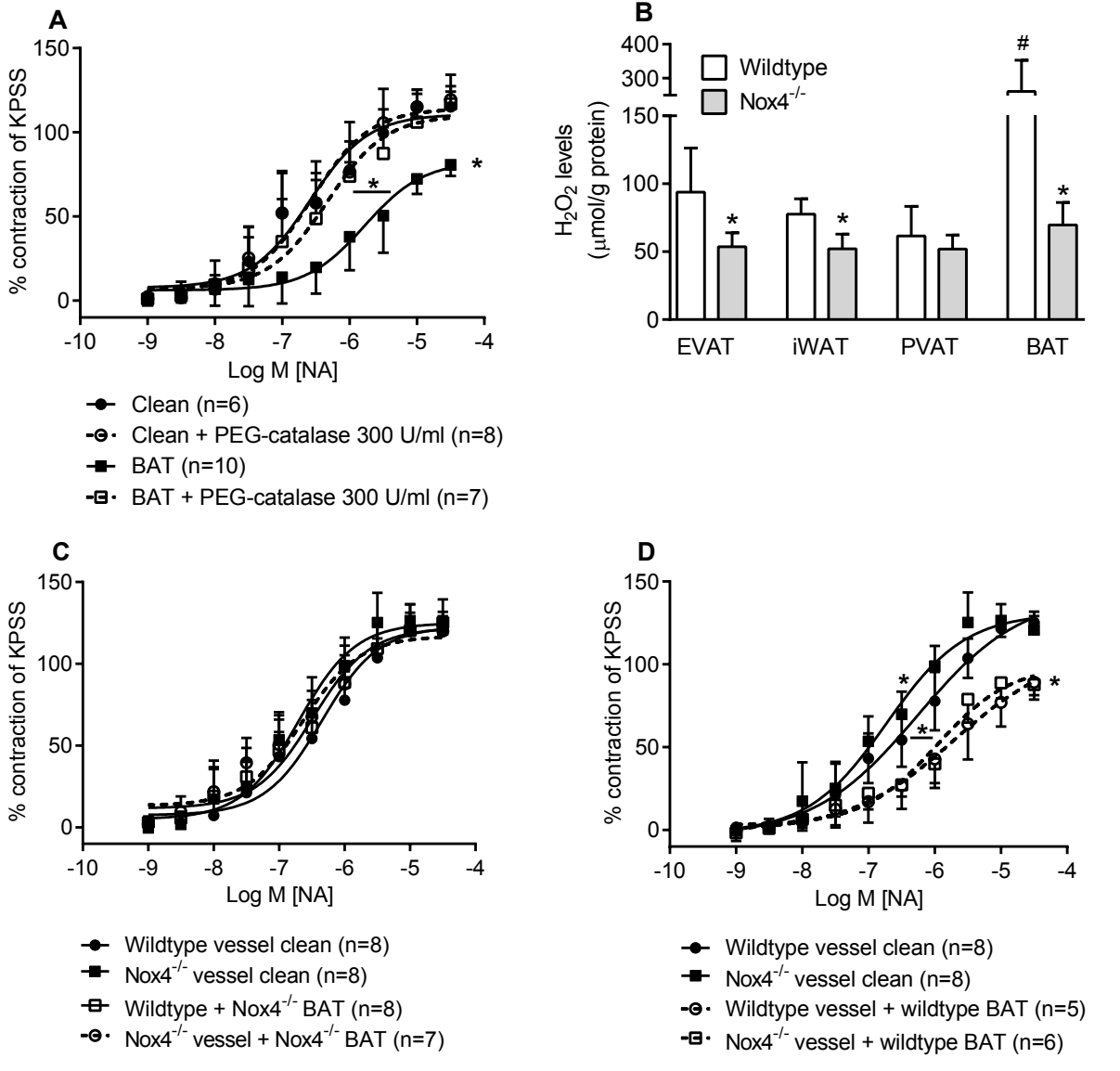
A
% contraction of KPSS
Log M [NA]
Clean (n=6)
Clean + PEG-catalase 300 U/ml (n=8)
BAT (n=10)
BAT + PEG-catalase 300 U/ml (n=7)
B
Wildtype
Nox4-/-
H2O2 levels (µmol/g protein)
EVAT
iWAT
PVAT
BAT
C
% contraction of KPSS
Log M [NA]
Wildtype vessel clean (n=8)
Nox4-/- vessel clean (n=8)
Wildtype + Nox4-/- BAT (n=8)
Nox4-/- vessel + Nox4-/- BAT (n=7)
D
% contraction of KPSS
Log M [NA]
Wildtype vessel clean (n=8)
Nox4-/- vessel clean (n=8)
Wildtype vessel + wildtype BAT (n=5)
Nox4-/- vessel + wildtype BAT (n=6)

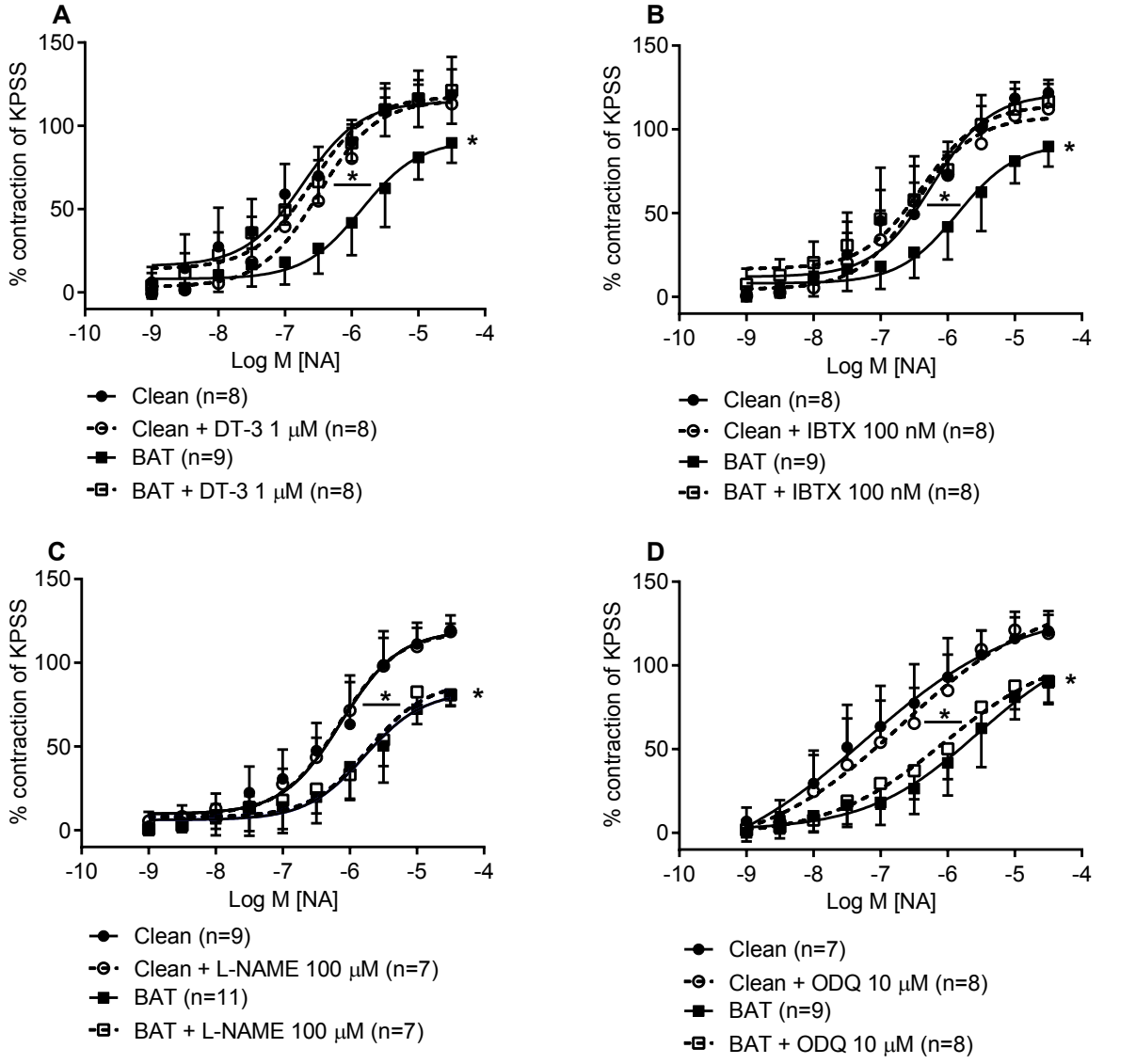
A
% contraction of KPSS
Log M [NA]
Clean (n=8)
Clean + DT-3 1 μM (n=8)
BAT (n=9)
BAT + DT-3 1 μM (n=8)
B
% contraction of KPSS
Log M [NA]
Clean (n=8)
Clean + IBTX 100 nM (n=8)
BAT (n=9)
BAT + IBTX 100 nM (n=8)
C
% contraction of KPSS
Log M [NA]
Clean (n=9)
Clean + L-NAME 100 μM (n=7)
BAT (n=11)
BAT + L-NAME 100 μM (n=7)
D
% contraction of KPSS
Log M [NA]
Clean (n=7)
Clean + ODQ 10 μM (n=8)
BAT (n=9)
BAT + ODQ 10 μM (n=8)

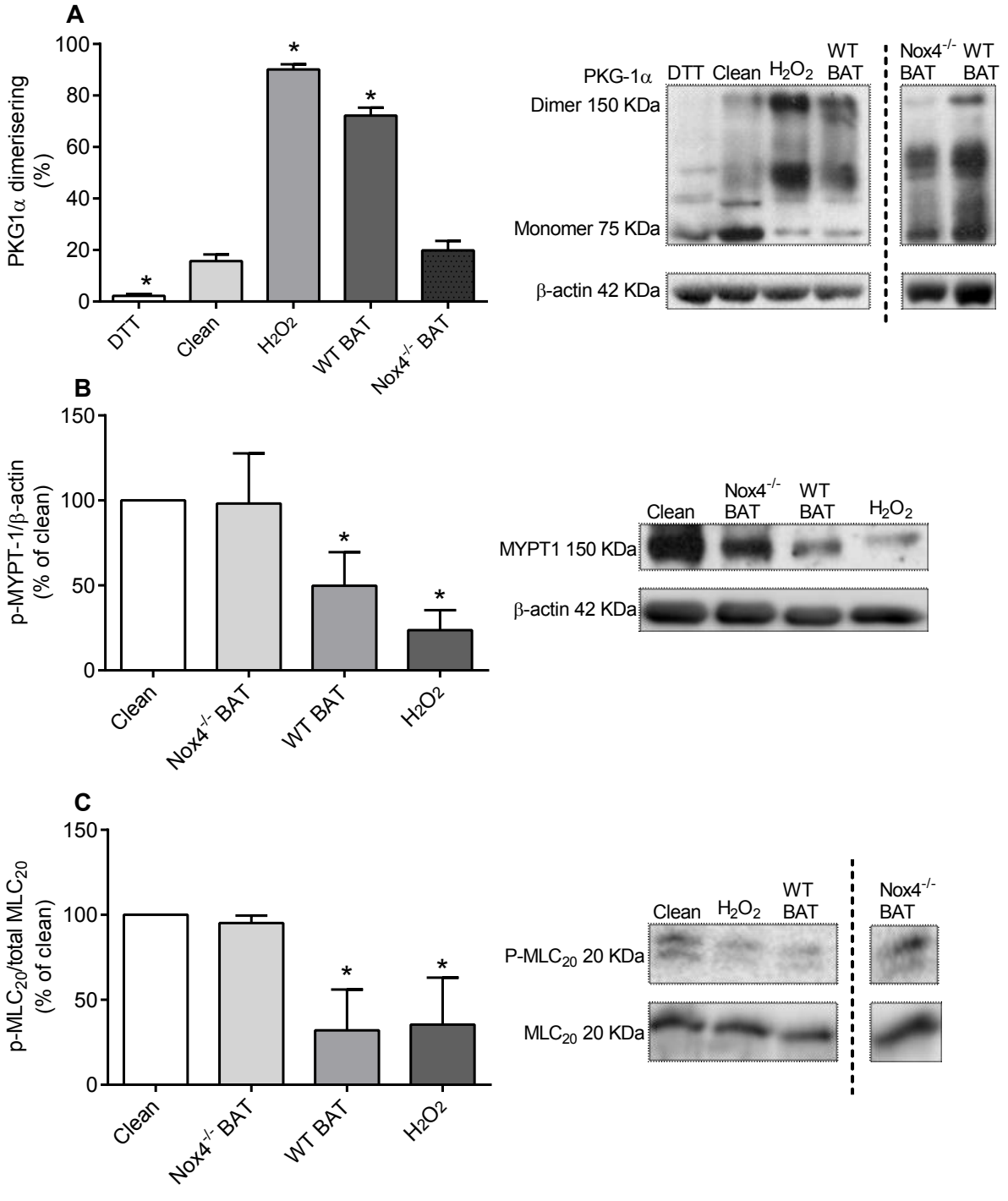
A
PKG1α dimerisering (%)
100
80
60
40
20
0
*
*
*
DTT
Clean
H2O2
WT BAT
Nox4-/- BAT
PKG-1α
DTT
Clean
H2O2
WT BAT
Nox4-/- BAT
WT BAT
Dimer 150 KDa
Monomer 75 KDa
β-actin 42 KDa
B
p-MYPT-1/β-actin (% of clean)
150
100
50
0
*
*
Clean
Nox4-/- BAT
WT BAT
H2O2
Clean
Nox4-/- BAT
WT BAT
H2O2
MYPT1 150 KDa
β-actin 42 KDa
C
p-MLC20/total MLC20 (% of clean)
150
100
50
0
*
*
Clean
Nox4-/- BAT
WT BAT
H2O2
Clean
H2O2
WT BAT
Nox4-/- BAT
P-MLC20 20 KDa
MLC20 20 KDa

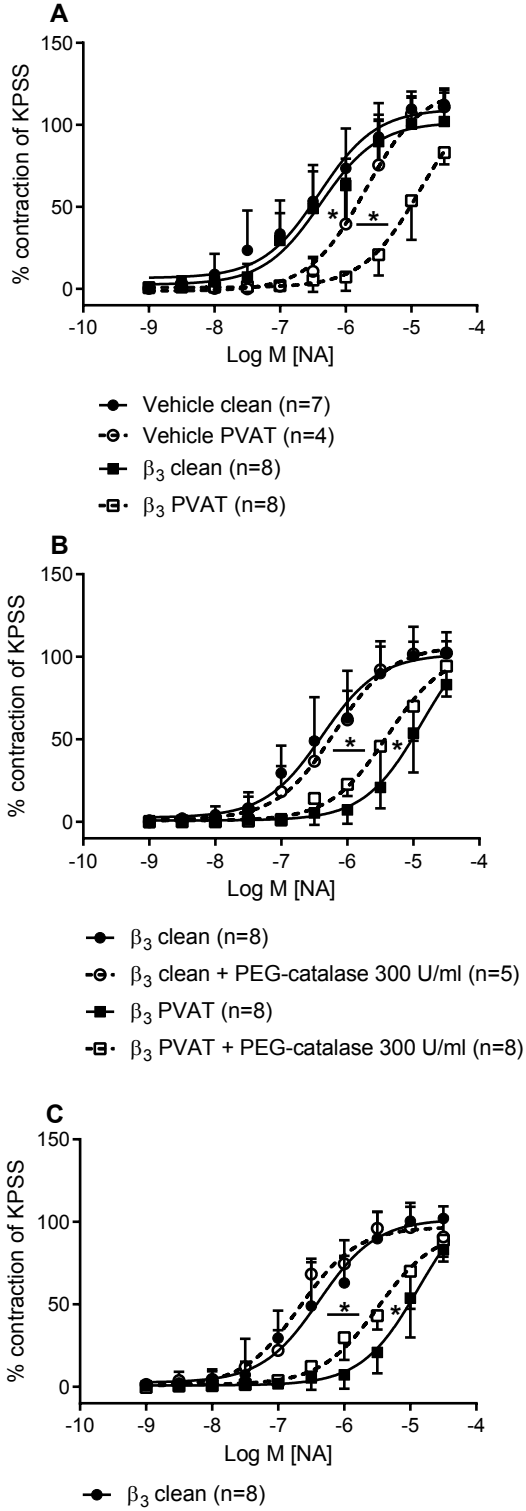
A
% contraction of KPSS
150
100
50
0
-10
-9
-8
-7
-6
-5
-4
Log M [NA]
*
*
Vehicle clean (n=7)
Vehicle PVAT (n=4)
β3 clean (n=8)
β3 PVAT (n=8)
B
% contraction of KPSS
150
100
50
0
-10
-9
-8
-7
-6
-5
-4
Log M [NA]
*
*
β3 clean (n=8)
β3 clean + PEG-catalase 300 U/ml (n=5)
β3 PVAT (n=8)
β3 PVAT + PEG-catalase 300 U/ml (n=8)
C
% contraction of KPSS
150
100
50
0
-10
-9
-8
-7
-6
-5
-4
Log M [NA]
*
*
β3 clean (n=8)
β3clean + DT-3 1 μM (n=5)
β3 PVAT (n=8)
β3PVAT + Dt-3 1 μM (n=9)

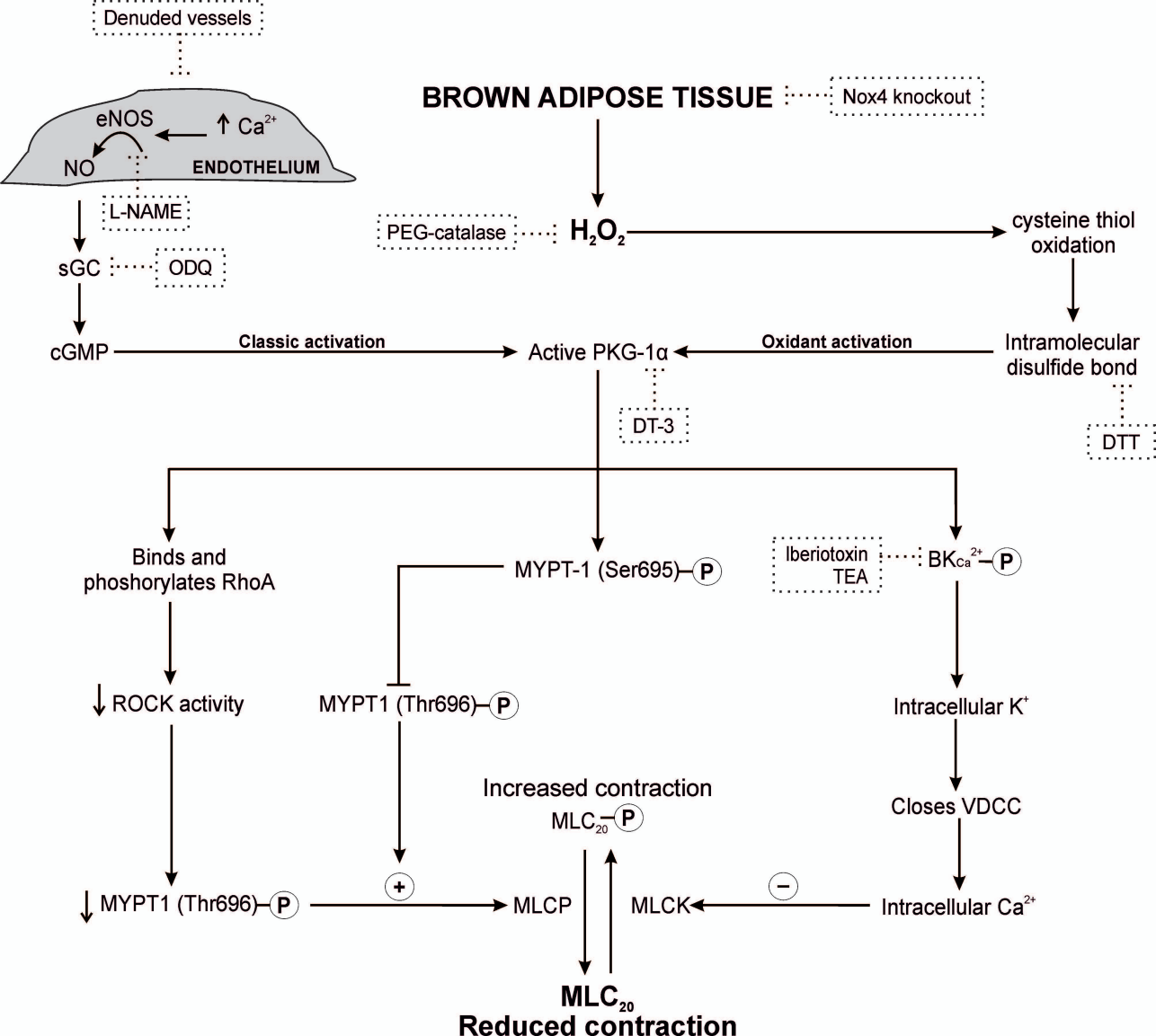
Denuded vessels
eNOS
↑ Ca2+
NO
ENDOTHELIUM
L-NAME
sGC
ODQ
BROWN ADIPOSE TISSUE
Nox4 knockout
PEG-catalase
H2O2
cysteine thiol oxidation
cGMP
Classic activation
Active PKG-1α
Oxidant activation
Intramolecular disulfide bond
DT-3
DTT
Binds and phoshorylates RhoA
MYPT-1 (Ser695)–P
Iberiotoxin TEA
BKCa2+–P
↓ ROCK activity
MYPT1 (Thr696)–P
Intracellular K+
Increased contraction
MLC20–P
Closes VDCC
↓ MYPT1 (Thr696)–P
+
MLCP
MLCK
–
Intracellular Ca2+
MLC20
Reduced contraction

SUPPLEMENTAL MATERIAL

Brown adipose tissue regulates small artery function through NADPH oxidase 4-derived hydrogen peroxide and redox-sensitive protein kinase G-1α.

Friederich-Persson M, Nguyen Dinh Cat A, Persson P, Montezano AC, Touyz RM.

Institute of Cardiovascular Medicine and Sciences, University of Glasgow, Glasgow, United Kingdom.

Supplementary table

Table 1. Mouse primer sequences for real time PCR.

Gene	Forward 5'-3'	Reverse 3'-5'
mSod1	GAGACCTGGGCAATGTGACT	TTGTTTCTCATGGACCACCA
mSod2	GGCCAAGGGAGATGTTACAA	GCTTGATAGCCTCCAGCAAC
mCatalase	ACATGGTCTGGGACTTCTGG	CAAGTTTTTGATGCCCTGGT
mFbx10	AAGTATGCCTCCAACCTGCC	TTTTTGGGGTGCTCGTCTGA
mUbc	GGTCAAACAGGAAGACAGACGTA	CACACCCAAGAACAAGCACA
mIpo8	ACCAGGACCCGTCACGTCG	ATCCACGGCAGGAGGTCGGT
mNox1	TCCCTTTGCTTCCTTCTTGA	CCAGCCAGTGAGGAAGAGTC
mNox2	CGCCCTTTGCCTCCATTCTC	CCTTTCCTGCATCTGGGTCTCC
mNox4	CCAGAATGAGGATCCCAGAA	AGCAGCAGCAGCATGTAGAA
mUcp-1	GGGCCCTTGTAAACAACAAA	GTCGGTCCTTCCTTGGTGTA
mTmem-26	GTGACCTGGGTGAAGGAAGA	TGCATTTCAAGAAGCCACAG
mLeptin	ATGTGCTGGAGACCCCTGTG	TCAGCATTCAGGGCTAACATCC
mCD137	CGTGCAGAACTCCTGTGATAAC	GTCCACCTATGCTGGAGAAGG
mP2Rx5	CTGCAGCTCACCATCCTGT	CACTCTGCAGGGAAGTGTCA
mPat2	ACAGGGATCCTCGGACTTC	GAGGCCCATTACCAGCAAG
mTbx1	GGCAGGCAGACGAATGTTC	TTGTCATCTACGGGCACAAAG
mTcf21	CATTCACCCAGTCAACCTGA	TTCCTTCAGGTCATTCTCTGG
mZiz1	AACCTCAAGATCCACAAAAGGA	CCTCGAACTCGCACTTGAA

CD137: tumor necrosis factor receptor superfamily member 9; FBX10: F-box and leucine-rich repeat protein-10; Ipo8: importin 8; m: mouse; Nox: NADPH oxidase;

Ubc: ubiquitin C; Ucp: uncoupling protein; P2RX5: purinergic Receptor P2X 5; Sod: superoxide dismutase; Tbx1: T-box protein 1; tcf21: transcription factor 21;Tmem-26: transmembrane protein 26; Zic1: Zinc finger of the cerebellum.

Supplemental figures and legends

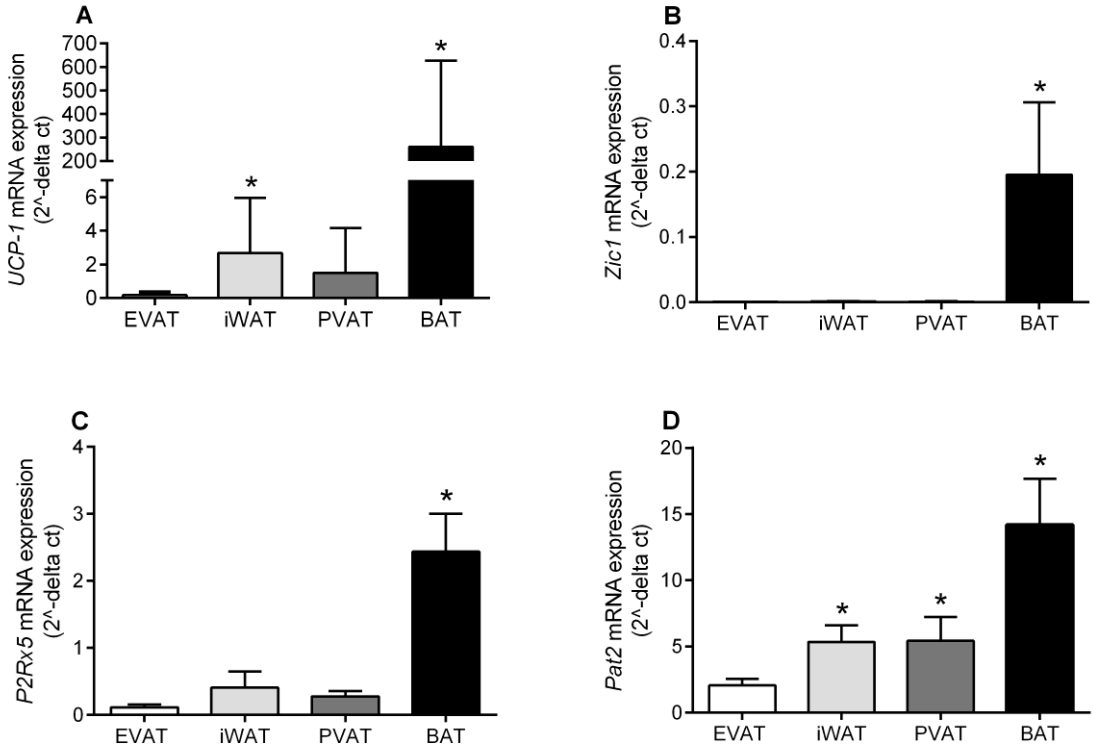

Supplemental Figure I. A) Joint BAT and BeAT marker *Ucp-1* is expressed in BAT and iWAT but at low levels in PVAT and EVAT. Specific BAT marker *Zic1* (B) and P2RX5 (C) is expressed in solely BAT. D) Joint BAT and BeAT marker Pat2 is expressed in iWAT, PVAT and BAT. Values are expressed as means±SD. N=6-8 animals per group. One-way ANOVA, followed by Bonferroni multiple comparison test, * P<0.05 vs. EVAT, BAT: brown adipose tissue; BeAT: beige adipose tissue; EVAT: epididymal visceral adipose tissue; iWAT: inguinal subcutaneous white adipose tissue; P2RX5: purinergic receptor 2X; PVAT: perivascular adipose tissue; Ucp-1: uncoupling protein 1; WAT: white adipose tissue; Zic: zinc finger of the cerebellum.

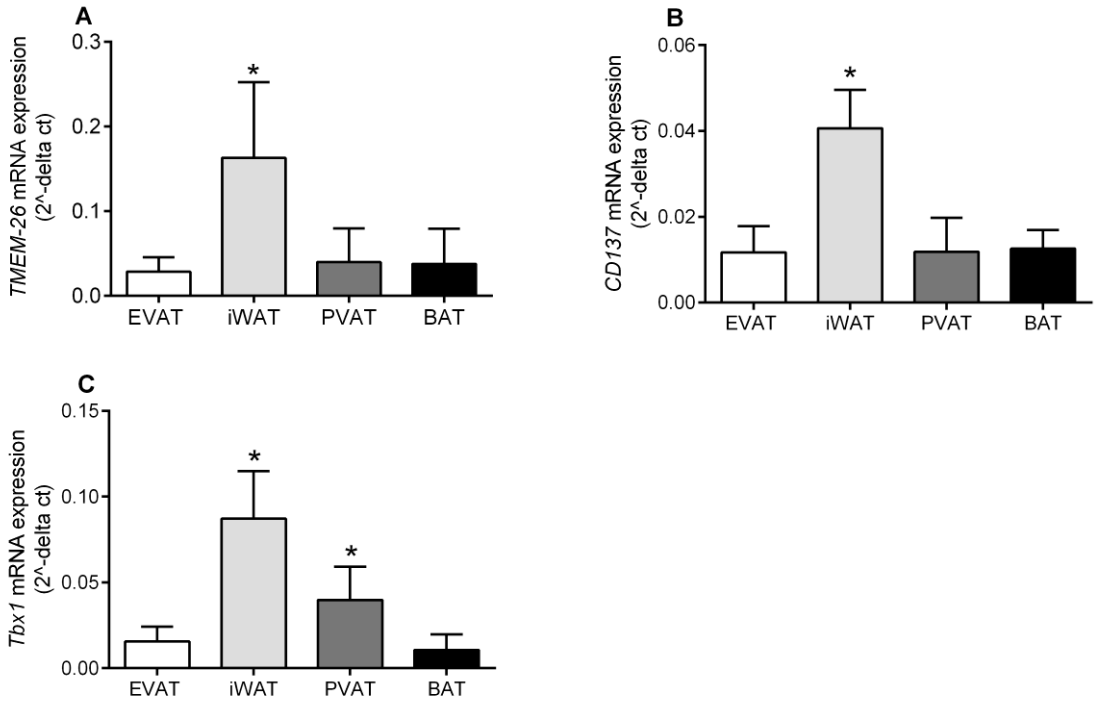

Supplemental Figure II. Specific BeAT markers *Tmem-26* (A) and *CD137* (B) are expressed in BAT and iWAT but at low levels in PVAT and EVAT. C) Specific BeAT marker *Tbx1*expressed in iWAT and PVAT. Values are expressed as means±SD. N=6-8 animals per group. One-way ANOVA, followed by Bonferroni multiple comparison test, * P<0.05 vs. EVAT, BAT: brown adipose tissue; BeAT: beige adipose tissue; EVAT: epididymal visceral adipose tissue; iWAT: inguinal subcutaneous white adipose tissue; PVAT: perivascular adipose tissue; Tbx: T-box protein; Tmem: transmembrane; WAT: white adipose tissue.

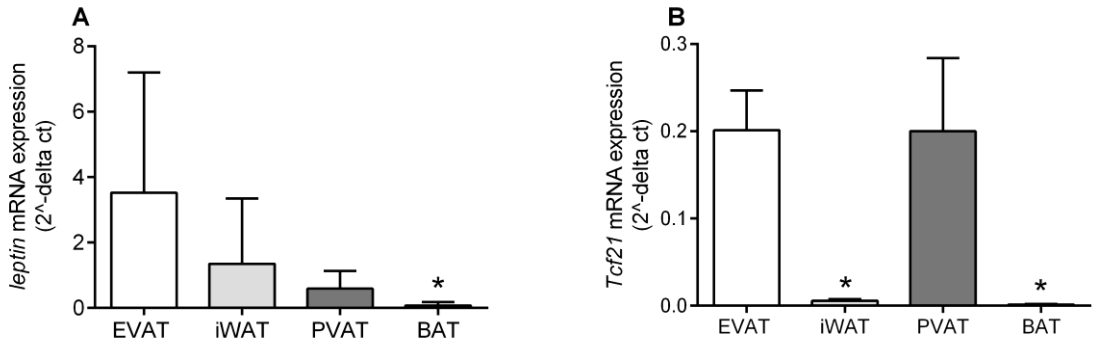

Supplemental Figure III. (A) WAT marker *leptin* is expressed in EVAT. B) Specific WAT marker *Tcf21* is expressed in EVAT and PVAT. Values are expressed as means±SD. N=6-8 animals per group. One-way ANOVA, followed by Bonferroni multiple comparison test, * P<0.05 vs. EVAT, BAT: brown adipose tissue; EVAT: epididymal visceral adipose tissue; iWAT: inguinal subcutaneous white adipose tissue; PVAT: perivascular adipose tissue; Tcf: transcription factor; WAT: white adipose tissue.

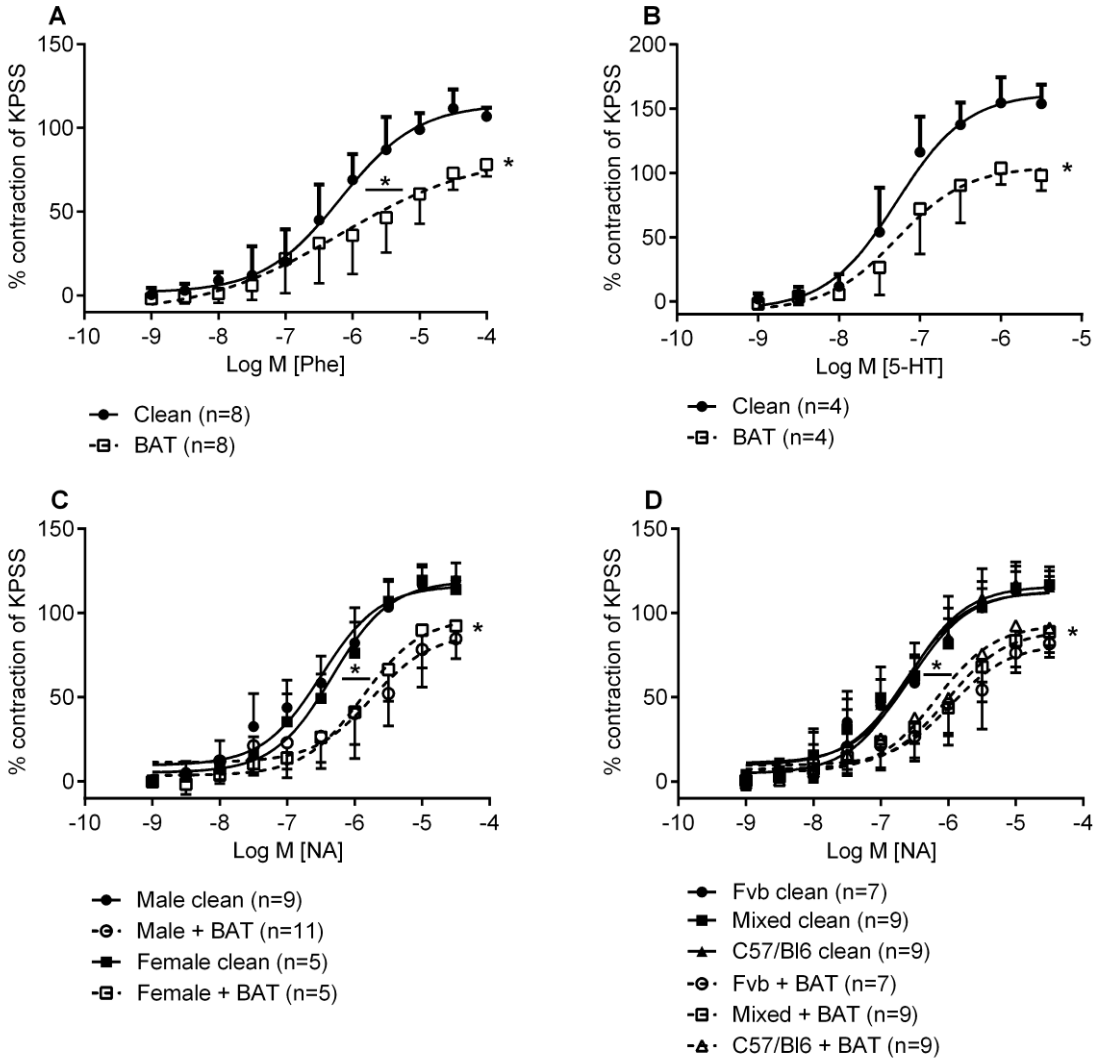

Supplemental Figure IV. The anticontractile effect of BAT is evident in response to both Phe (A, 2by2 interaction: ns) and 5-HT (B, 2by2 interaction: ns). The anticontractile effect of BAT is similar regardless of gender (C, 2by2 interaction: ns) and strain (D (2by2 interaction: ns). Values are expressed as means ± SD. In brackets are indicated the number of animals per group. Repeated measured two-way ANOVA, followed by Bonferroni multiple comparison test, * P<0.05 vs clean vessels. 5-HT: 5-hydroxytryptamine; BAT: brown adipose tissue; NA: noradrenaline; KPSS: potassium-rich physiological saline solution; Phe: phenylephrine.

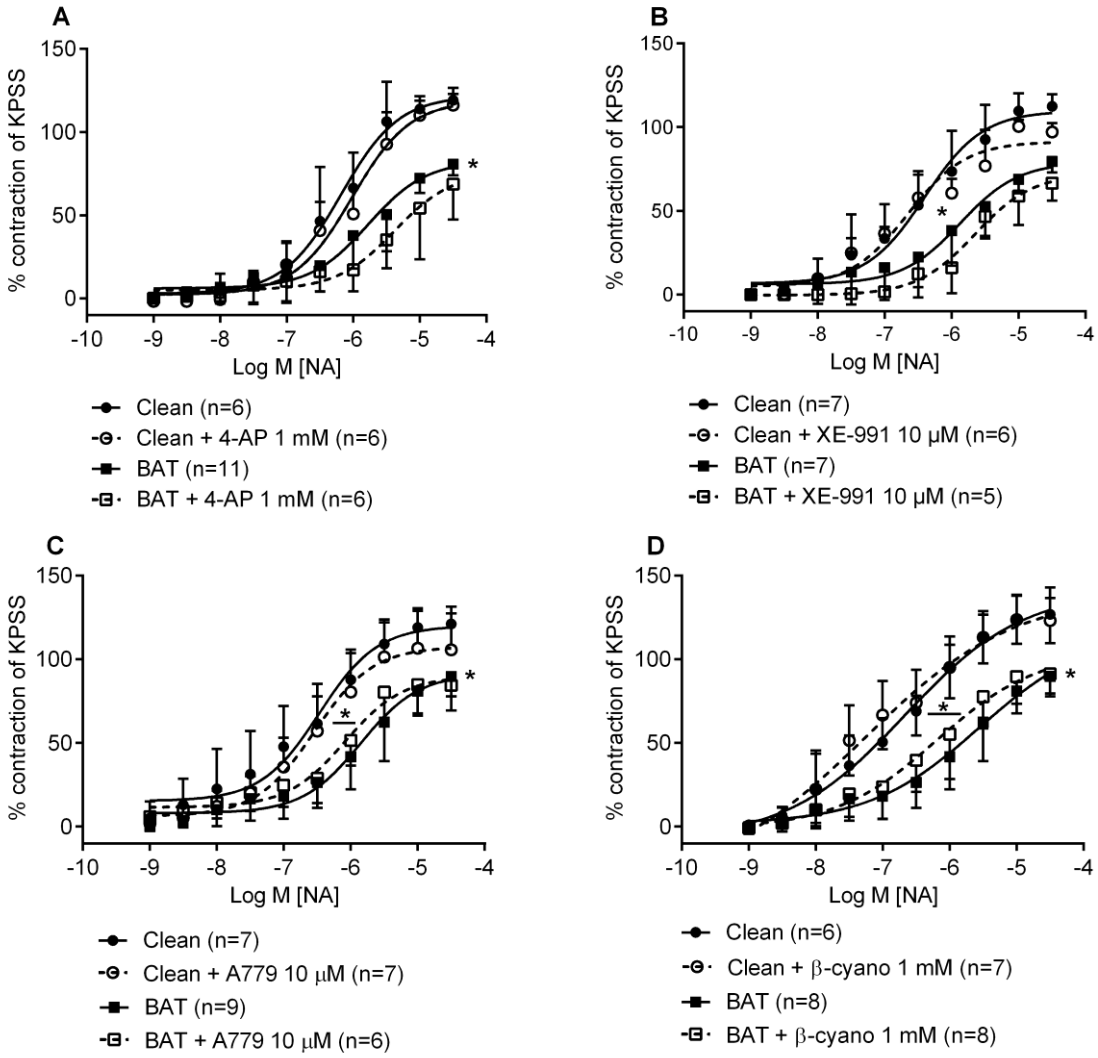

Supplemental Figure V. The anticontractile effect of BAT is not affected by voltage-gated K-channels by 4-AP blockade (A, 2by2 interaction: $p<0.05$) or XE-991 (B, 2by2 interaction: $p<0.05$), angiotensin 1-7 receptor blockade by A779 (C, 2by2 interaction: ns) or blockage of γ-cystathione lyase (producer of H_2S) inhibition by β-cyanoalanine (β-cyano) (D, 2by2 interaction: ns). Values are expressed as means ± SD. In brackets are indicated the number of animals per group. Repeated measured two-way ANOVA, followed by Bonferroni multiple comparison test, * $P<0.05$ vs. clean vessels. 4-AP: 4-aminopyridine; β-cyano: β-cyanoalanine; BAT: brown adipose tissue; H_2S; hydrogen sulphide; KPSS: potassium-rich physiological saline solution; NA: noradrenaline.

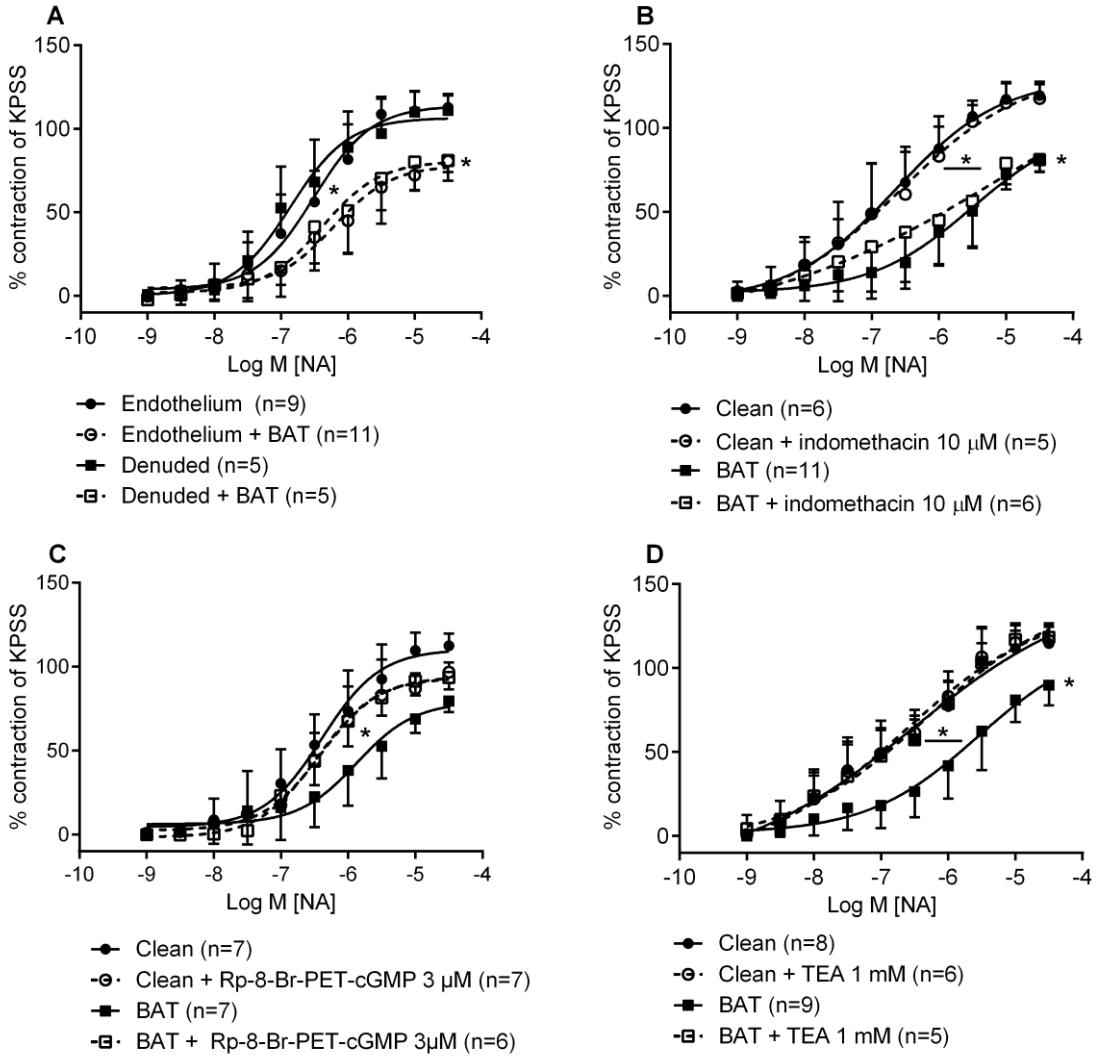

Supplemental Figure VI. The anticontractile effect of BAT is not affected by removal of the endothelium (A, 2by2 interaction: ns), indomethacin (B, 2by2 interaction: ns). The anticontractile effect was blocked by PKG-inhibitor Rp-8-Br-PET-cGMP (C, 2by2 interaction: $p<0.05$) and calcium-sensitive potassium channel blocker TEA (D, 2by2 interaction: $p<0.05$). Values are expressed as means ± SD. In brackets are indicated the number of animals per group. Repeated measured two-way ANOVA, followed by Bonferroni multiple comparison test, * $P<0.05$ vs. clean vessels. BAT: brown adipose tissue; KPSS: potassium-rich physiological saline solution; NA: noradrenaline; PKG: protein kinase G; TEA: tetraethylammonium.

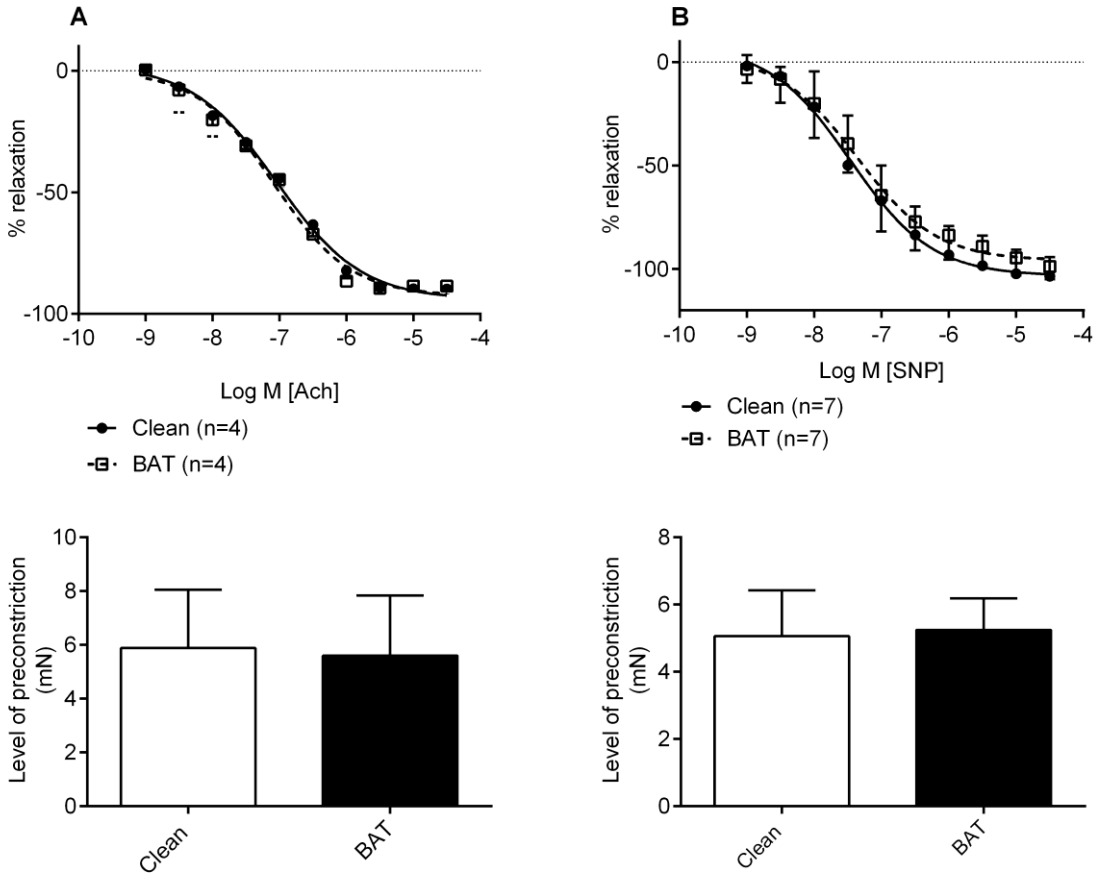

Supplemental Figure VII. A) BAT does not affect endothelium-dependent relaxation in response to ACh. B) BAT does not affect endothelium-independent relaxation in response to SNP. Values are expressed as means ± SD. In brackets are indicated the number of animals per group. Bar graphs show level of preconstriction in response to NA. ACh: acetylcholine; BAT: brown adipose tissue; KPSS: potassium-rich physiological saline solution; NA: noradrenaline; SNP: sodium nitroprusside.

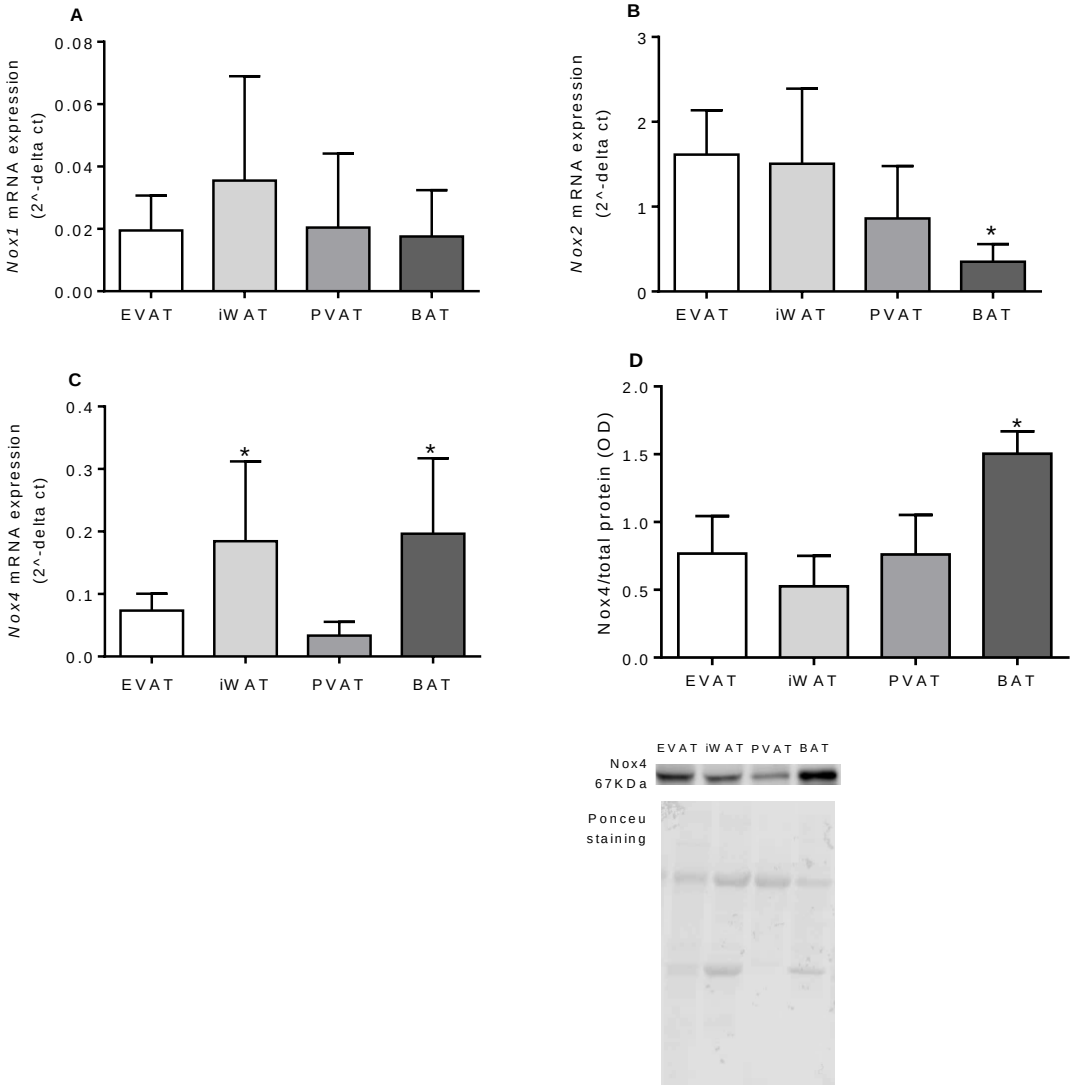

Supplemental Figure VIII. Figure 2. A) Nox1 expression does not vary between adipose depots. B) Nox2 expression is decreased in BAT. C) Nox4 is increased in iWAT and BAT. D) Nox 4 protein level is increased in BAT. Values are expressed as means ± SD. A-C: n=8 animals per group, D: n=3-7 per group. One-way ANOVA, followed by Bonferroni multiple comparison test, * P<0.05 vs. EVAT. BAT: brown adipose tissue; EVAT: epididymal visceral adipose tissue; iWAT: inguinal white adipose tissue; PVAT: perivascular adipose tissue.

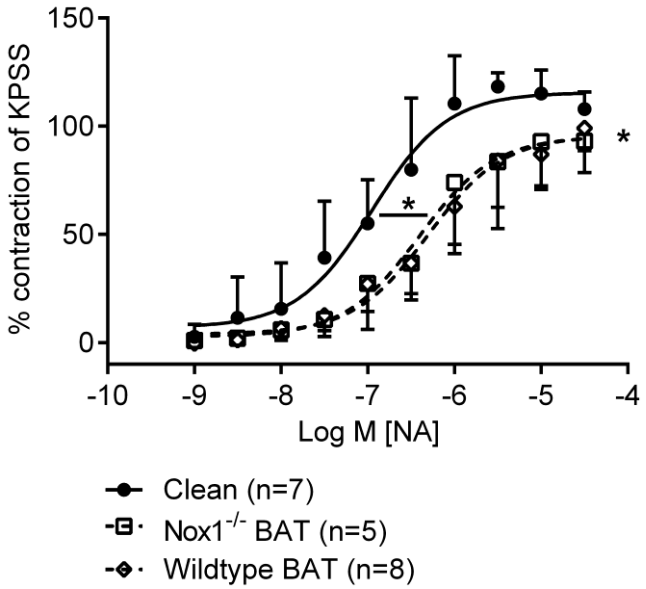

Supplemental Figure IX. BAT from Nox1$^{-/-}$ mice exerts a similar anticontractile effect as BAT from wildtype mice. Values are expressed as means ± SD. In brackets are indicated the number of animals per group. One-way ANOVA, followed by Bonferroni multiple comparison test, * P<0.05 vs. clean vessels. BAT: brown adipose tissue; KPSS: potassium-rich physiological saline solution; NA: noradrenaline; Nox: NADPH oxidase.

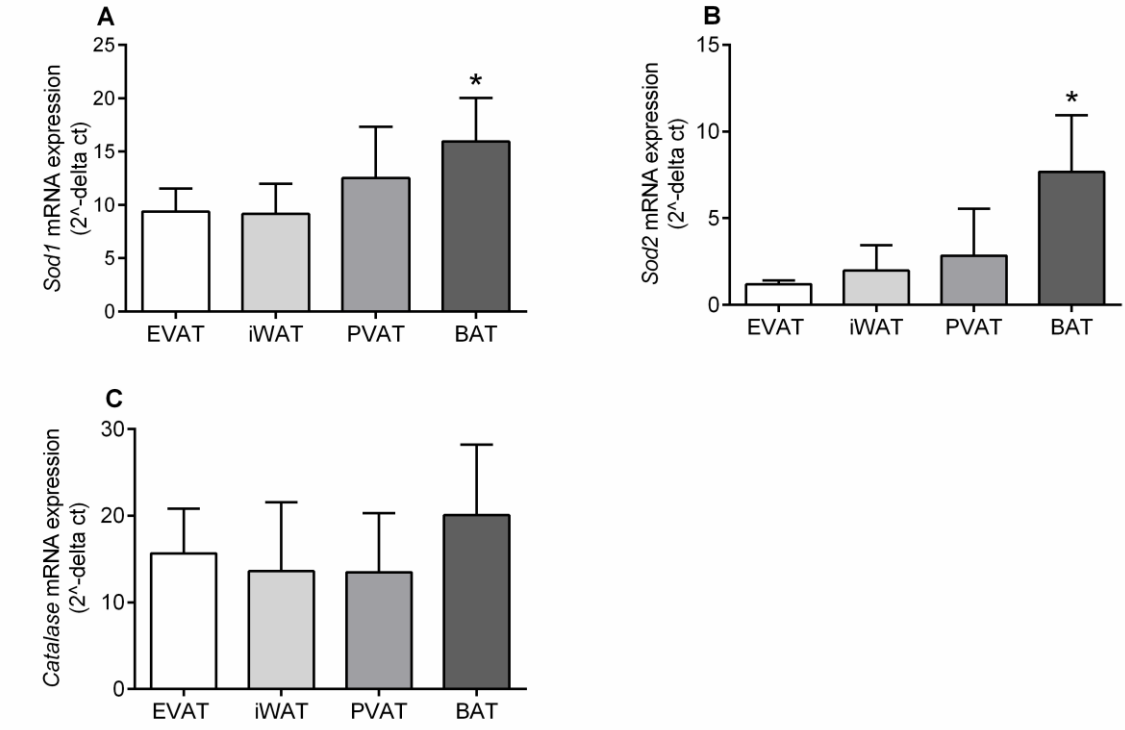

Supplemental Figure X. BAT displayed increased mRNA levels of *Sod1* (A) and *Sod2* (B). *Catalase* mRNA levels were not changed between adipose depots (C). Values are expressed as means ± SD. n=8 animals per group. One-way ANOVA, followed by Bonferroni multiple comparison test, * P<0.05 vs EVAT. BAT: brown adipose tissue; EVAT: epididymal visceral adipose tissue; iWAT: inguinal subcutaneous white adipose tissue; PVAT: perivascular adipose tissue; Sod: superoxide dismutase.

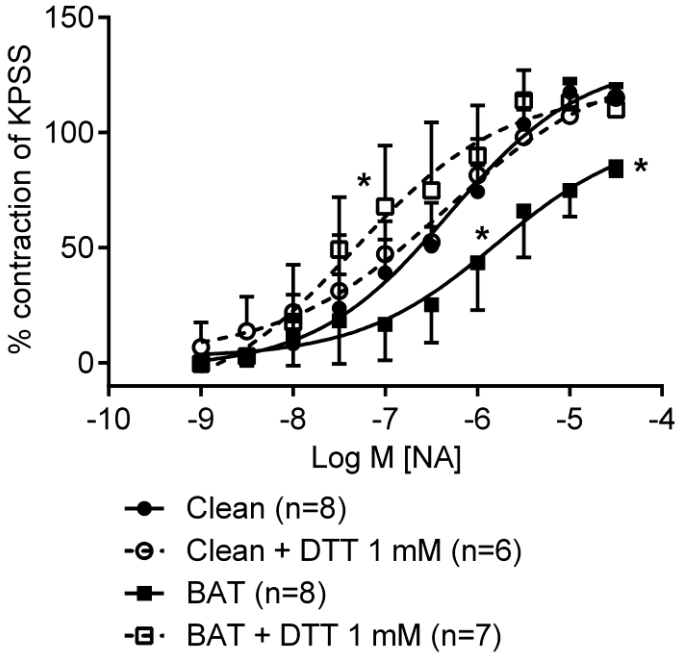

Supplemental Figure XI. DTT prevents the anticontractile effect of BAT. Values are expressed as means ± SD. In brackets are indicated the number of animals per group. Repeated measured two-way ANOVA, followed by Bonferroni multiple comparison test, * P<0.05 vs. clean vessels, 2by2 interaction: p<0.05. BAT: brown adipose tissue; DTT: dithiotreitol; KPSS: potassium-rich physiological saline solution; NA: noradrenaline.

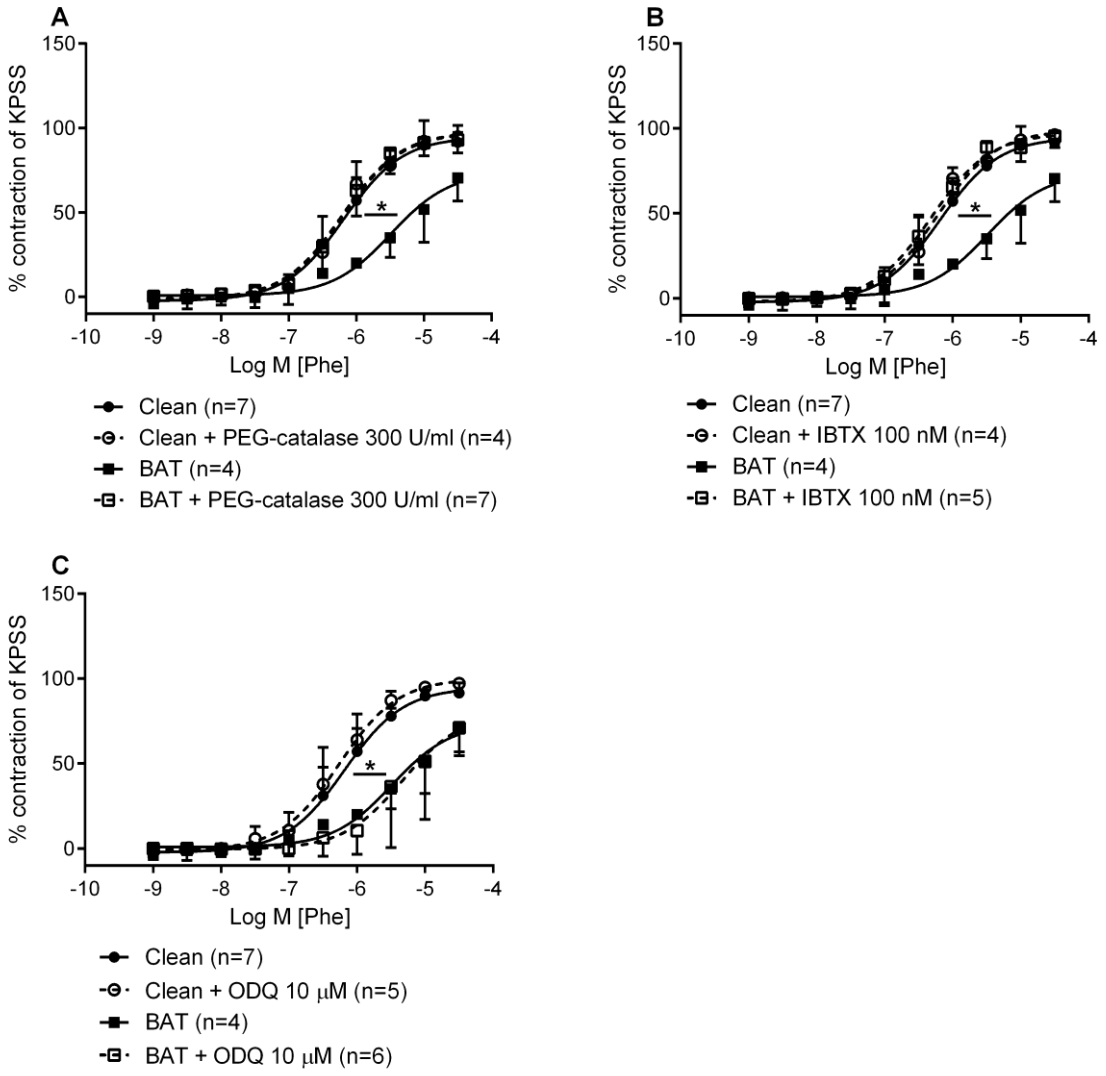

Supplemental Figure XII. Using phenylephrine as the contractile agent, the anticontractile effect of BAT is removed by PEG-catalase (A, 2by2 interaction: $p<0.05$) and IBTX (B, 2by2 interaction: $p<0.05$) but not by ODQ (C, 2by2 interaction: ns). Values are expressed as means ± SD. In brackets are indicated the number of animals per group. Repeated measured two-way ANOVA, followed by Bonferroni multiple comparison test, * $P<0.05$ vs. clean vessels. BAT: brown adipose tissue; IBTX: iberiotoxin; KPSS: potassium-rich physiological saline solution; PEG: polyethyleneglykol; Phe: phenylephrine.

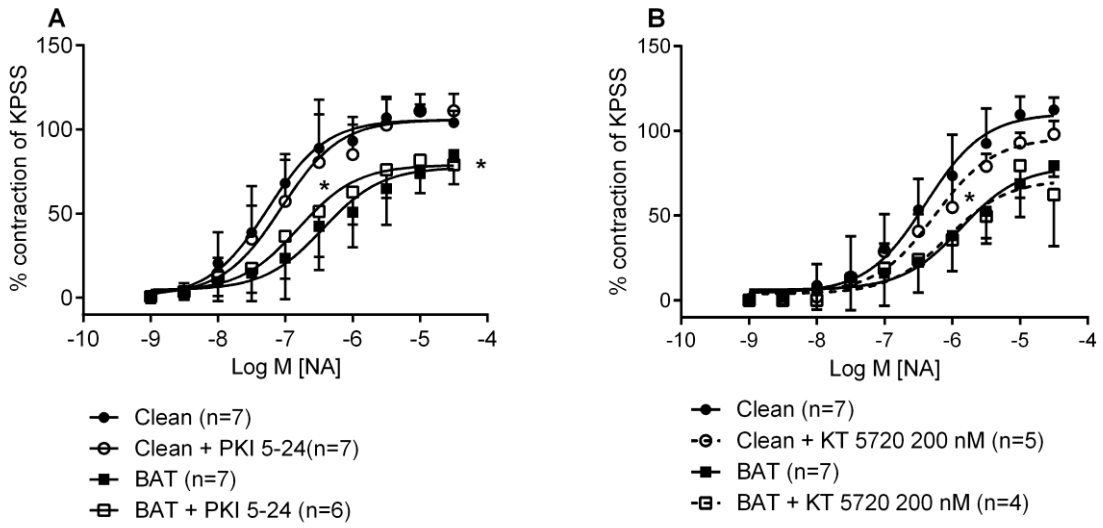

Supplemental Figure XIII. Protein kinase A inhibition by PKI 5-24 (A, 2by2 interaction:ns) or KT-5720 (B, 2by2 interaction: $p<0.05$) does not affect the anticontractile effect of BAT. Values are expressed as means ± SD. In brackets are indicated the number of animals per group. Repeated measured two-way ANOVA, followed by Bonferroni multiple comparison test, * $P<0.05$ vs clean vessels. BAT: brown adipose tissue; KPSS: potassium-rich physiological saline solution; NA: noradrenaline.

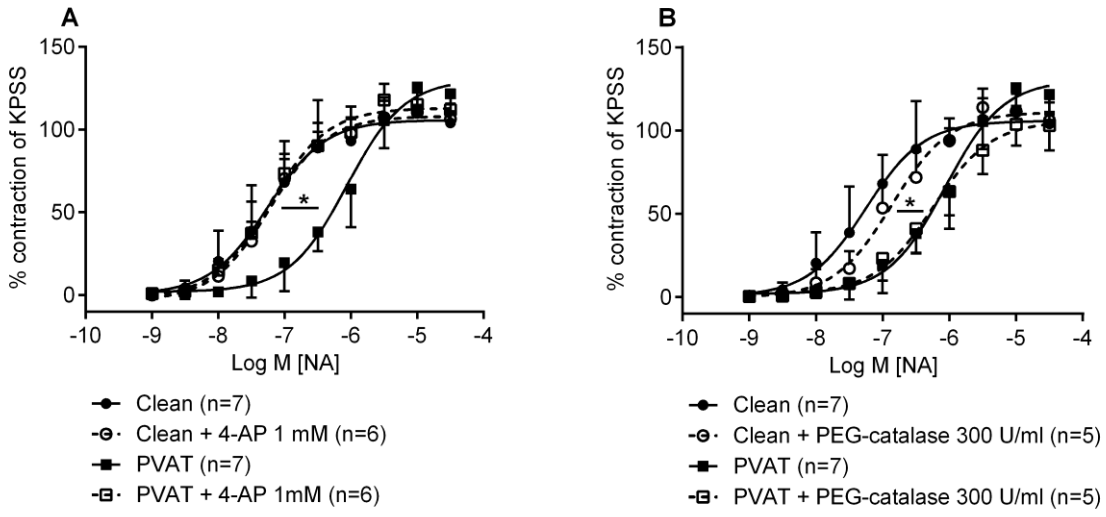

Supplemental Figure XIV. The anticontractile effect of mesenteric PVAT is prevented after blockade of Kv-channels (A, 2by2 interaction: $p<0.05$) and not affected by H_2O_2 scavenging by PEG-catalase (B, 2by2 interaction: ns). Values are expressed as means ± SD. In brackets are indicated the number of animals per group. Repeated measured two-way ANOVA, followed by Bonferroni multiple comparison test, * $P<0.05$ vs. clean. 4-AP: 4-aminopyridine; BAT: brown adipose tissue; KPSS: potassium-rich physiological saline solution; Kv-channel: voltage gated potassium-channel; PEG: polyethylene glycated; PVAT: perivascular adipose tissue.

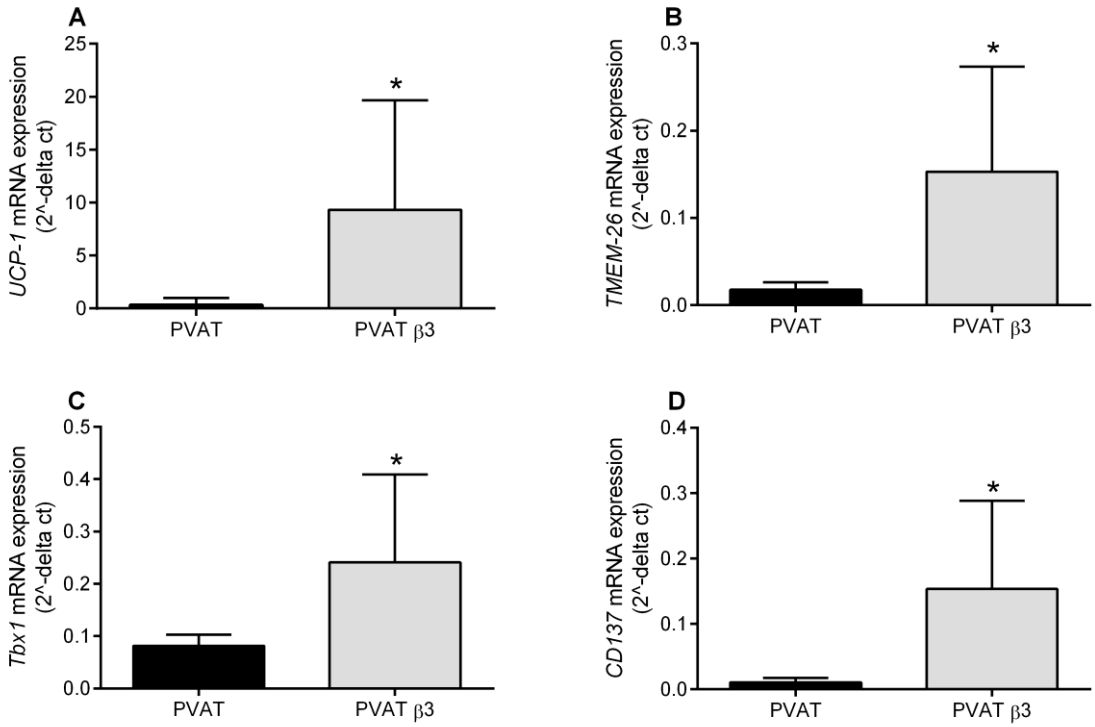

Supplemental Figure XV. Mesenteric PVAT obtained from mice treated with β_3-agonist CI-316,243 display increased of joint BAT and BeAT marker *Ucp1* (A) as well as specific BeAT markers *tmem-26* (B)*, Tbx1* (B) and *CD137 (*D). Values are displayed as mean ± SD, N=5-7 per group. * P<0.05 vs PVAT, Student's t-test. BAT: brown adipose tissue; BeAT: beige adipose tissue; PVAT: perivascular adipose tissue; tbx: T-box protein; tmem: transmembrane protein; ucp: uncoupling protein.